HIERARCHICAL MULTI-STAGE RECOVERY FRAMEWORK FOR KRONECKER COMPRESSED SENSING

Anonymous authors
Paper under double-blind review

ABSTRACT

In this paper, we study the Kronecker compressed sensing problem, which focuses on recovering sparse vectors using linear measurements obtained using the Kronecker product of two or more matrices. We first introduce the *hierarchical view* of the Kronecker compressed sensing, showing that the Kronecker product measurement matrix probes the sparse vector from different levels, following a block-wise and hierarchical structure. Leveraging this insight, we develop a versatile multi-stage sparse recovery algorithmic framework and tailor it to three different sparsity models: standard, hierarchical, and Kronecker-supported. We further analyze the restricted isometry property of Kronecker product matrices under different sparsity models, and provide theoretical recovery guarantees for our multi-stage algorithm. Simulations demonstrate that our method achieves comparable recovery performance to other state-of-the-art techniques while substantially reducing run time owing to the hierarchical, multi-stage recovery process.

1 INTRODUCTION

Kronecker compressed sensing (KCS) is a measurement framework that employs the Kronecker product of multiple factor matrices as a measurement matrix, capturing multidimensional signal structure while reducing measurement complexity. It appears in many acquisition systems, such as sensor arrays in communication systems (He & Joseph, 2025a) or separable filters in imaging (Friedland et al., 2014). We focus on the general KCS problem with canonical form,

$$\boldsymbol{y} = \boldsymbol{H}\boldsymbol{x} + \boldsymbol{n} = (\boldsymbol{H}_I \otimes \boldsymbol{H}_{I-1} \otimes \cdots \otimes \boldsymbol{H}_1)\,\boldsymbol{x} + \boldsymbol{n} = \left(\otimes_{i=I}^{1} \boldsymbol{H}_i\right)\boldsymbol{x} + \boldsymbol{n}. \tag{1}$$

Here, $\boldsymbol{x} \in \mathbb{R}^{\bar{N}}$ is the *unknown* sparse vector and $\boldsymbol{y} \in \mathbb{R}^{\bar{M}}$ is the noisy measurements via a *known* measurement matrix $\boldsymbol{H} = \otimes_{i=I}^{1} \boldsymbol{H}_i$, where each factor matrix $\boldsymbol{H}_i \in \mathbb{R}^{M_i \times N_i}$ has *full row rank*.

A key challenge in solving Equation 1 is the high dimensionality of the multidimensional signal $\boldsymbol{x}$. It grows rapidly with both the number and size of factor matrices $\boldsymbol{H}_i$, e.g., $\mathcal{O}(N^I)$ if $N_i = \mathcal{O}(N)$. Another challenge is exploiting sparsity patterns as prior knowledge. Beyond simple sparsity, the nonzero elements in $\boldsymbol{x}$ often exhibit more complex but regulated patterns. We consider three prevalent models. The first model is the standard sparsity, where the nonzero entries can be positioned arbitrarily. This model is ubiquitous and tied to various applications, such as image processing (Duarte & Baraniuk, 2010; Li & Bernal, 2017; Zhao et al., 2019), system identification (Sun et al., 2022; Yuan et al., 2019), regression (Ament & Gomes, 2021), and communications (Berger et al., 2010; Xiao et al., 2024). The second model, hierarchical sparsity, considers a vector $\boldsymbol{x}$ partitioned into blocks at multiple levels, and sparsity is structured across these levels. For example, in massive machine-type communication (Wunder et al., 2017; Roth et al., 2018; 2020), only a subset of devices are active (device-level sparsity), and each active device sends a sparse signal, forming a two-level hierarchical structured sparsity pattern on $\boldsymbol{x}$. The third model, Kronecker-supported sparsity (or the block tensor sparsity) (He & Joseph, 2025a; 2023; Caiafa & Cichocki, 2013; Zhao et al., 2019; Boyer & Haardt, 2016), assumes the support of $\boldsymbol{x}$ is the Kronecker product of multiple binary support vectors. This pattern arises in radar imaging and wireless communications, where signals are separable across dimensions (He & Joseph, 2023; Xu et al., 2022; He & Joseph, 2025d). Motivated by varied sparsity patterns, we focus on efficient methods for KCS with structured sparsity.

This paper introduces a novel *hierarchical view* on KCS, showing how its dimension-wise measuring structure can be used to design and analyze efficient recovery methods to exploit structured sparsity efficiently. Our main contributions are as follows:

- *Hierarchical View*: We establish that when measuring via Kronecker product matrices, each factor matrix in the Kronecker product captures the vector at a distinct hierarchical level. It provides a unified perspective for handling different sparsity models within a single framework.
- *Unified Algorithm*: We design a multi-stage sparse recovery algorithm using the hierarchical view. By leveraging the Kronecker structure of $\boldsymbol{H}$ through tensor operation and investigating the underlying structure, our method achieves a significant complexity reduction, e.g., reducing from $\mathcal{O}((MN)^I)$ (He & Joseph, 2025a) to $\mathcal{O}(MN^I)$ regarding Kronecker-supported sparse vector recovery, and accommodates the mentioned sparsity patterns within a single, flexible framework.
- *Theoretical Guarantees*: We establish a unified restricted isometry property (RIP) analysis for KCS covering the standard, hierarchical, and Kronecker-supported sparsity. It proves that sparsity at each hierarchical level, rather than total sparsity, drives the recovery. Our result improves the RIP-based bound for KCS with standard sparsity and provides a cohesive understanding of structured sparsity. We also provide a RIP-based recovery guarantee for our unified algorithm.

Related works: The Kronecker product measurement matrix is introduced for compressed imaging in Rivenson & Stern (2009). KCS is formalized in Duarte & Baraniuk (2011a) with an RIP analysis for KCS with standard sparsity (Duarte & Baraniuk, 2011a;b). It bounds the restricted isometry constant (RIC) of the Kronecker product using the RIC of factor matrices $\boldsymbol{H}_i$. However, the recovery algorithm fails to leverage the Kronecker structure in $\boldsymbol{H}$. To leverage this structure, Kronecker orthogonal matching pursuit (KroOMP) (Caiafa & Cichocki, 2013) adopts tensor operations. Nonetheless, it still incurs a high complexity of $\mathcal{O}(N^I)$, and lacks theoretical analysis. In parallel, Friedland et al. (2014; 2015) presents two algorithms: one uses tensor unfolding for sequential recovery in dimension, and the other uses approximate Tucker decomposition to recover along each dimension. Still, both approaches are limited to standard sparsity. Later, Li & Bernal (2017) decomposes the unfolding-based approach into multiple *independent* subproblems. Yet, it fails to exploit joint sparsity patterns and is not immediately extendable to other sparsity patterns.

Structured sparse recovery is also investigated in the literature, but seldom under the KCS framework. For *hierarchically sparse* vectors, Roth et al. (2020) discusses the hierarchical hard thresholding pursuit (HiHTP), adapting classic hard thresholding pursuit (HTP) with a tailored RIP and coherence analysis. However, it fails to incorporate the Kronecker structure in $\boldsymbol{H}$, leading to higher computational costs. For *Kronecker-supported sparsity*, both greedy and Bayesian methods have been explored. An orthogonal matching pursuit (OMP)-based algorithm offers reduced complexity (Caiafa & Cichocki, 2012; Caiafa & Cichocki, 2013) but performs poorly in noisy settings (He & Joseph, 2025a). Bayesian algorithms, designed for applications such as hyperspectral image processing (Zhao et al., 2019) and wireless communication (He & Joseph, 2025a; Chang & Su, 2021; Xu et al., 2022), use a structured prior distribution. They suffer from poor generalization and high complexity (He & Joseph, 2025b). Besides, both OMP-based and Bayesian algorithms lack theoretical guarantees. Recently, He & Joseph (2025c) provides an algorithm and RIP analysis for KCS for the $I = 2$ case. However, the analysis is decoupled from the algorithm. Also, it relies heavily on specific matrix properties, making the generalization to higher orders ($I > 2$) nontrivial.

To summarize, existing approaches reveal several literature gaps. First, KCS methods mostly ignore the structures of $\boldsymbol{H}$, relying on generic solvers, while our method is specifically designed to leverage the Kronecker structure through tensor operations. Second, current methods are largely tailored to a single sparsity pattern and cannot be generalized, whereas our work provides a unified framework for multiple patterns. Third, many methods suffer from high computational complexity, while our approach is efficient and low-complexity. Besides, no prior work offers a unified RIP analysis of Kronecker-structured matrices across different sparsity patterns, nor a recovery framework for different sparsity patterns with RIP-based guarantees, which are our central theoretical contributions.

Notation and tensor preliminaries: We use $[I]$ to denote the set $\{1, 2, \cdots, I\}$ for any scalar I and $\boldsymbol{I}_N$ to denote the $N \times N$ identity matrix. The symbols $\otimes$ and $\times_j$ denote Kronecker and jth mode product, respectively. The jth mode unfolding $\boldsymbol{T}_{(j)}$ of tensor $\mathbf{T} \in \mathbb{R}^{N_1 \times N_2 \times \cdots \times N_I}$ is $\left[\boldsymbol{T}_{(j)}\right]_{n_j,k} = [\mathbf{T}]_{n_1,n_2,\ldots,n_I}$ for $j \in [I]$ with $k = 1 + \sum_{\ell=1,\ell\neq j}^{I} \left(\prod_{p=1,p\neq j}^{\ell-1} N_p\right)(n_l - 1)$, with $n_j \in [N_j]$. Also, $[\boldsymbol{T}_{(j)}]_{n_j,k}$ is (n_j, k)th matrix entry, and $[\mathbf{T}]_{n_1,n_2,\cdots,n_I}$ is the $(n_1, \cdots, n_I)$th tensor entry. The ith mode product of $\boldsymbol{D}_i \in \mathbb{R}^{N_i \times M_i}$ with $\mathbf{T}$ is $\mathbf{M} = \mathbf{T} \times_i \boldsymbol{D}_i \in \mathbb{R}^{M_1 \times \cdots \times M_{i-1} \times N_i \times M_{i+1} \times \cdots \times M_I}$. The ith mode unfolding of $\mathbf{M}$ is $\boldsymbol{M}_{(i)} = \boldsymbol{D}_i \boldsymbol{T}_{(i)}$ (Kolda & Bader, 2009).

2 HIERARCHICAL VIEW OF THE KRONECKER-STRUCTURED MEASURING

Our hierarchical view builds on the Kronecker structure in Equation 1, interpreting the measurement matrix as probing the signal's sparsity across multiple block-wise and hierarchical levels. To illustrate this, we first introduce the hierarchical block partition of a sparse vector $\boldsymbol{x} \in \mathbb{R}^{\bar{N}}$.

Hierarchical partition: We first partition $\boldsymbol{x}$ in Equation 1 into N_I equal-length blocks, denoting the Ith level blocks as $\{\boldsymbol{x}_{(n_I)}\}_{n_I=1}^{N_I} \in \mathbb{R}^{\prod_{i=1}^{I-1} N_i}$. Each $\boldsymbol{x}_{(n_I)}$ is further partitioned into N_{I-1} blocks, denoted as $(I-1)$th level blocks $\{\boldsymbol{x}_{(n_{I-1},n_I)}\}_{n_{I-1}=1}^{N_{I-1}} \in \mathbb{R}^{\prod_{i=1}^{I-2} N_i}$. We continue until we reach blocks of length N_1 at the second level. The first-level blocks are the individual entries of $\boldsymbol{x}$.

For brevity, we use $\boldsymbol{x}_{\mathrm{n_j}}$ to denote a block in the jth level with length $\prod_{i=1}^{j-1} N_i$ and encapsulation $\mathrm{n_j} := (n_j, \cdots, n_{I-1}, n_I)$. An encapsulation $\mathrm{n_j} := (n_j, \cdots, n_{I-1}, n_I)$ can be viewed as a coordinate for blocks in this hierarchical block structure. Also, set $[\![\boldsymbol{x}_{\mathrm{n_j}}]\!]$ contains all N_j *child blocks* that share the same parent block at the level $j+1$ as that of $\boldsymbol{x}_{\mathrm{n_j}}$. We illustrate a hierarchical partition for $\boldsymbol{x} \in \mathbb{R}^{40}$ in Figure 1, where $[\![\boldsymbol{x}_{(1,3)}]\!] = [\![\boldsymbol{x}_{(2,3)}]\!] = \{\boldsymbol{x}_{(1,3)}, \boldsymbol{x}_{(2,3)}\}$ as they share the parent $\boldsymbol{x}_{(3)}$.

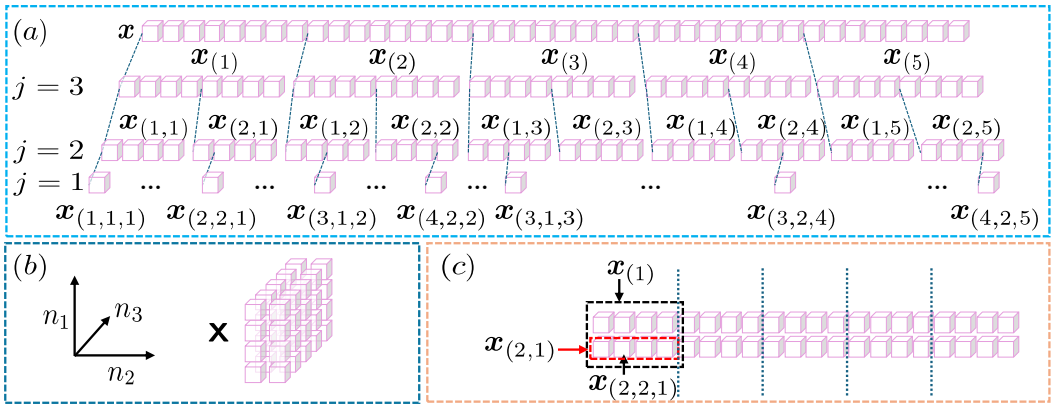

Figure 1: (a) Hierarchical partition for $\boldsymbol{x} \in \mathbb{R}^{40}$ with $I = 3, N_1 = 5, N_2 = 2, N_1 = 4$, and $\bar{N} = 40$. (b) Reordered tensor $\mathbf{X}$. (c) Mode unfolding $\boldsymbol{X}_{(2)}$ and the relation between the n_{I-1}th row within the n_Ith column block and the $(I-1)$th level child block $\boldsymbol{x}_{n_{\mathrm{I}-1}}$ with $n_{\mathrm{I}-1} = (2,1)$ and $I = 3$.

Hierarchical view: We first focus on the noiseless version of Equation 1 reformulated using tensors,

$$\mathbf{T} := \mathbf{Y} = \mathbf{X} \times_1 \boldsymbol{H}_1 \cdots \times_I \boldsymbol{H}_I,$$

where the first mode unfolding satisfy $\mathrm{vec}(\boldsymbol{X}_{(1)}) = \boldsymbol{x}$ and $\mathrm{vec}(\boldsymbol{T}_{(1)}) = \mathrm{vec}(\boldsymbol{Y}_{(1)}) = \boldsymbol{y}$. Unfolding $\mathbf{T}$ on the Ith mode leads to

$$\boldsymbol{T}_{(I)} = \boldsymbol{H}_I \boldsymbol{X}_{(I)} \left(\otimes_{i=I-1}^{1} \boldsymbol{H}_i^\top\right) = \boldsymbol{H}_I \boldsymbol{U}_I \in \mathbb{R}^{M_I \times \prod_{i=I-1}^{I} M_i}.$$

Here, $\boldsymbol{U}_I = \boldsymbol{X}_{(I)} \left(\otimes_{i=I-1}^{1} \boldsymbol{H}_i^\top\right) \in \mathbb{R}^{N_I \times \prod_{i=I-1}^{I} M_i}$ and $\boldsymbol{X}_{(I)} \in \mathbb{R}^{N_I \times \prod_{i=I-1}^{I} N_i}$ whose n_Ith row is the Ith level block $\boldsymbol{x}_{\mathrm{n_I}}$ with $\mathrm{n_I} = (n_I)$. Therefore, matrix $\boldsymbol{H}_I$ acts on $\boldsymbol{U}_I$, and a zero row in $\boldsymbol{U}_I$ indicates that the corresponding Ith level block is entirely zero. Hence, matrix $\boldsymbol{H}_I$ captures the sparsity pattern of the Ith-level blocks.

For the $(I-1)$th level, we fold $\boldsymbol{U}_I$ into a new tensor $\mathbf{T}$, whose Ith mode unfolding $\boldsymbol{T}_{(I)} = \boldsymbol{U}_I$, as

$$\mathbf{T} = \mathbf{X} \times_1 \boldsymbol{H}_1 \cdots \times_{I-1} \boldsymbol{H}_{I-1} \times_I \boldsymbol{I}_{N_I}.$$

Unfolding $\mathbf{T}$ along its $(I-1)$th mode gives

$$\boldsymbol{T}_{(I-1)} = \boldsymbol{H}_{I-1} \boldsymbol{X}_{(I-1)} \left(\boldsymbol{I}_{N_I} \otimes \left(\otimes_{i=I-2}^{1} \boldsymbol{H}_i^\top\right)\right) = \boldsymbol{H}_{I-1} \boldsymbol{U}_{I-1} \in \mathbb{R}^{M_{I-1} \times N_I \prod_{i=I-2}^{I} M_i}.$$

Here, $\boldsymbol{X}_{(I-1)} \in \mathbb{R}^{N_{I-1} \times \bar{N}/N_{I-1}}$ has N_I column blocks, with n_Ith block corresponding to $\boldsymbol{x}_{\mathrm{n_I}}$ with $\mathrm{n_I} = (n_I)$. Within the n_Ith column block, the n_{I-1}th row is the $(I-1)$th level child block $\boldsymbol{x}_{n_{\mathrm{I}-1}}$ with $n_{\mathrm{I}-1} = (n_{I-1}, n_I)$, as illustrated in Figure 1c. The Kronecker product $\boldsymbol{I}_{N_I} \otimes \left(\otimes_{i=I-2}^{1} \boldsymbol{H}_i^\top\right)$

is a block matrix and preserves the column block structure in $\boldsymbol{U}_{I-1}$. Column blocks of $\boldsymbol{U}_{I-1}$ are associated with I-level blocks, and the rows of a column block correspond to the $(I-1)$ level blocks. Hence, the zero rows in each column block of $\boldsymbol{U}_{I-1}$ indicate that the corresponding $(I-1)$th level blocks are entirely zero. Therefore, $\boldsymbol{H}_{I-1}$ captures the sparsity pattern at the $(I-1)$th-level blocks.

For a general jth level, we define $\mathsf{T} = \mathsf{X} \times_1 \boldsymbol{H}_1 \times_2 \boldsymbol{H}_2 \cdots \times_j \boldsymbol{H}_j \times_{j+1} \boldsymbol{I}_{N_{j+1}} \cdots \times_I \boldsymbol{I}_{N_I}$, and

$$\boldsymbol{T}_{(j)} = \boldsymbol{H}_j \boldsymbol{X}_{(j)} \left(\boldsymbol{I}_{\prod_{i=I}^{j+1} N_i} \otimes \left(\otimes_{i=j-1}^{1} \boldsymbol{H}_i \right) \right)^\top \in \mathbb{R}^{M_j \times \prod_{i=I}^{j+1} N_i \prod_{i=j-1}^{1} M_i},$$

is its jth unfolding. Similar to the column block structure at $(I-1)$th level, we have the following.

Lemma 1. *Consider a sparse tensor X reordered from a sparse vector $\boldsymbol{x}$ such that $\mathrm{vec}(\boldsymbol{X}_{(1)}) = \boldsymbol{x}$. For the jth mode unfolding of X, i.e., $\boldsymbol{X}_{(j)}$, and with full row rank $\boldsymbol{H}_i$'s, the matrix*

$$\boldsymbol{U}_j := \boldsymbol{X}_{(j)} \left(\boldsymbol{I}_{\prod_{i=I}^{j+1} N_i} \otimes \left(\otimes_{i=j-1}^{1} \boldsymbol{H}_i \right) \right)^\top \in \mathbb{R}^{N_j \times \prod_{i=I}^{j+1} N_i \prod_{i=j-1}^{1} M_i},$$

can be divided into $\prod_{i=I}^{j+1} N_i$ column blocks. Each block is indexed by an encapsulation $\mathrm{n_{j+1}}$ with $\mathrm{n_{j+1}} = (n_{j+1}, \cdots, n_I)$ for $n_k \in [N_k]$ for $k = j+1, \ldots, I$. The number of nonzero rows in a column block indexed by $\mathrm{n_{j+1}}$ equals the number of nonzero blocks in $[\![\boldsymbol{x}_{\mathrm{n_j}}]\!]$ with $\mathrm{n_j} = (n_j, n_{j+1}, \cdots, n_I)$.

Lemma 1 implies that matrix $\boldsymbol{H}_j$ actually captures the sparsity at the jth level blocks, which we refer to as the *hierarchical view* of KCS. The above perspective can also be interpreted directly from Equation 1. The Kronecker product matrix $\boldsymbol{H}$ has a recursive column-block structure: each block of columns is obtained by taking the Kronecker product of a column of $\boldsymbol{H}_I$ with $\otimes_{i=I-1}^{1} \boldsymbol{H}_i$, which itself has a column block structure. This recursive structure aligns with the hierarchical partition block of $\boldsymbol{x}$. Hence, in this hierarchical framework, factor matrices $\{\boldsymbol{H}_i\}_{i=I}^{1}$ operate at different levels: for any p, q with $p > q$, $\boldsymbol{H}_q$ first measures each qth level block of $\boldsymbol{x}$, the resulting measurements of all blocks are then processed by $\boldsymbol{H}_p$, which captures sparsity at a higher level.

3 Multi-Stage Sparse Recovery Algorithm

We aim to recover $\boldsymbol{x}$ in Equation 1 from noisy measurement $\boldsymbol{y}$, given $\{\boldsymbol{H}_i\}_{i=1}^{I}$. Guided by the hierarchical view in Section 2, we next present a recovery framework that handles each $\boldsymbol{H}_i$ sequentially. We formally define the following three considered sparsity models.

Sparsity 1 (Standard sparsity)**.** *A vector $\boldsymbol{x} \in \mathbb{R}^{\bar{N}}$ is s sparse if $\boldsymbol{x}$ contains at most s nonzeros.*

Sparsity 2 (Hierarchical sparsity)**.** *A vector $\boldsymbol{x} \in \mathbb{R}^{\bar{N}}$ is $\boldsymbol{s}$ hierarchically sparse with $\boldsymbol{s} := (s_I, s_{I-1}, \cdots, s_1)$ if it has a hierarchical partition defined by $\{N_j\}_{j=1}^{I}$, and at each level $j \in [I]$, every set $[\![\boldsymbol{x}_{\mathrm{n_j}}]\!]$ contains at most s_i nonzero blocks.*

Sparsity 3 (Kronecker-supported sparsity)**.** *A vector $\boldsymbol{x} \in \mathbb{R}^{\bar{N}}$ is $\boldsymbol{s}$ Kronecker supported sparse if its support is the Kronecker product of s_i sparse support vectors $\boldsymbol{b}_j \in \{0,1\}^{N_j}$ for $j \in [I]$.*

We note that the Kronecker-supported sparsity is a special case of hierarchical sparsity, where at each level $j \in [I]$, the s_j nonzero blocks $\boldsymbol{x}_{\mathrm{n_j}}$ share the same support.

Our framework first solves for $\boldsymbol{U}_I = \boldsymbol{X}_{(I)} \left(\otimes_{i=I-1}^{1} \boldsymbol{H}_i \right)^\top$ from unfolding along Ith mode using

$$\boldsymbol{T}_{(I)} := \boldsymbol{Y}_{(I)} = \boldsymbol{H}_I \boldsymbol{U}_I + \boldsymbol{N}_{(I)}. \tag{2}$$

Here, $\boldsymbol{U}_I$ exhibits a row sparsity pattern where a zero row in $\boldsymbol{U}_I$ corresponds to an all-zero Ith level block $\boldsymbol{x}_{\mathrm{n_I}}$. Thus, recovering $\boldsymbol{U}_I$ from Equation 2 is a multiple measurement vector (MMV) problem and solved using MMV algorithms such as simultaneous OMP (SOMP), simultaneous iterative hard thresholding (SIHT), simultaneous HTP (SHTP), or MMV sparse Bayesian learning (MMV-SBL).

Let the estimate of $\boldsymbol{U}_I$ be $\tilde{\boldsymbol{U}}_I$ with error $\boldsymbol{E}_I$ modeling the estimation error and residual noise, $\tilde{\boldsymbol{U}}_I = \boldsymbol{U}_I + \boldsymbol{E}_I$. In the second step, we treat $\tilde{\boldsymbol{U}}_I$ as the noisy measurement and $\boldsymbol{E}_I$ as noise, reorder them into tensor T and N such that $\mathsf{T}_{(I)} = \tilde{\boldsymbol{U}}_I$ and $\mathsf{N}_{(I)} = \boldsymbol{E}_I$, to obtain $\mathsf{T} = \mathsf{X} \times_1 \boldsymbol{H}_1 \cdots \times_{I-1} \boldsymbol{H}_{I-1} \times_I \boldsymbol{I}_{N_I} + \mathsf{N}$. Unfolding T along its $(I-1)$th mode as

$$\boldsymbol{T}_{(I-1)} = \boldsymbol{H}_{I-1} \boldsymbol{U}_{I-1} + \boldsymbol{N}_{(I-1)}. \tag{3}$$

For standard and hierarchical sparsity models, the supports of different $(I-1)$th level blocks of $\boldsymbol{x}$ are different. By Lemma 1, zero $(I-1)$th level blocks leads to the zero rows in each column block in $\boldsymbol{U}_{I-1}$, making it a concatenation of N_I row sparse matrices $[\boldsymbol{U}_{I-1}]_{\mathrm{n_I}} := [\boldsymbol{X}_{(I-1)}]_{\mathrm{n_I}} \left(\otimes_{i=I-2}^{1} \boldsymbol{H}_i\right)^\top$ for $\mathrm{n_I} = (n_I)$ and $n_I \in [N_I]$. We thus partition Equation 3 into N_I independent MMV problems as

$$[\boldsymbol{T}_{(I-1)}]_{\mathrm{n_I}} = \boldsymbol{H}_{I-1}[\boldsymbol{U}_{I-1}]_{\mathrm{n_I}} + [\boldsymbol{N}_{(I-1)}]_{\mathrm{n_I}},$$

and solve them (sequentially or in parallel) using MMV solvers. Concatenating estimates $\tilde{\boldsymbol{U}}_{I-1} := [[\tilde{\boldsymbol{U}}_{I-1}]_1, [\tilde{\boldsymbol{U}}_{I-1}]_2, \cdots, [\tilde{\boldsymbol{U}}_{I-1}]_{N_I}]$ gives the final solution, where $[\tilde{\boldsymbol{U}}_{I-1}]_{\mathrm{n_I}} = [\boldsymbol{U}_{I-1}]_{\mathrm{n_I}} + [\boldsymbol{E}_{I-1}]_{\mathrm{n_I}}$. However, for the Kronecker-supported sparsity, Equation 3 is a single MMV problem because the support is common across the $(I-1)$th level blocks.

Generalizing, for jth mode unfolding step, with measurement $\tilde{\boldsymbol{U}}_{j+1}$ from the previous step,

$$\tilde{\boldsymbol{U}}_{j+1} = \boldsymbol{U}_{j+1} + \boldsymbol{E}_{j+1} = \boldsymbol{X}_{(j+1)} \left(\boldsymbol{I}_{\prod_{i=I}^{j+2} N_i} \otimes \left(\otimes_{i=j}^{1} \boldsymbol{H}_i\right)\right)^\top + \boldsymbol{E}_{j+1}. \tag{4}$$

We unfold the measurement tensor formed from $\tilde{\boldsymbol{U}}_{j+1}$ along its jth mode as

$$\boldsymbol{T}_{(j)} = \boldsymbol{H}_j \boldsymbol{U}_j + \boldsymbol{N}_{(j)}. \tag{5}$$

Lemma 1 reduces Equation 5 to $\prod_{i=I}^{j+1} N_i$ independent MMV problems for standard and hierarchical sparsity. Sparsity varies across MMVs for the standard model (defined via the total sparsity, not level-wise sparsity) but remains identical in the hierarchical model. For Kronecker-supported sparsity, Equation 5 is a single MMV due to shared block support. While mixed models with single and multiple MMVs at different levels are possible, we focus on these three main cases for brevity, leading to the Multi-Stage Recovery (MSR) algorithm, summarized in Algorithm 1.

Algorithm 1 Multi-Stage Recovery (MSR)

Input: Measurement $\boldsymbol{y}$, dictionaries $\{\boldsymbol{H}_i\}_{i=1}^{I} \in \mathbb{R}^{M_i \times N_i}$
1: Fold $\boldsymbol{y}$ to $\mathbf{Y}$ according to the dimensions of dictionaries $\{\boldsymbol{H}_i\}_{i=1}^{I}$, and initialize $\mathbf{T} = \mathbf{Y}$
2: **for** $j = I, I-1, \cdots, 1$ **do**
3: Obtain the jth mode unfolding of $\mathbf{T}$, i.e., $\boldsymbol{T}_{(j)}$
4: Solve Equation 5 for $\boldsymbol{U}_j$ via a compressed sensing algorithm to get estimate $\tilde{\boldsymbol{U}}_j$
5: Fold $\tilde{\boldsymbol{U}}_j$ back to $\mathbf{T}$ such that the jth mode unfolding of $\mathbf{T}$, i.e., $\boldsymbol{T}_{(j)}$ is $\tilde{\boldsymbol{U}}_j$
6: **end for**
Output: Estimated sparse vector $\hat{\boldsymbol{x}} = \mathrm{vec}(\tilde{\boldsymbol{U}}_1)$

Complexity: We compare the complexity of MSR variants with existing methods for each sparsity model, assuming Equation 5 is solved sequentially, and $M_i = \mathcal{O}(M)$, $N_i = \mathcal{O}(N)$ for $i \in [I]$ with $I < M < N$. For standard sparsity, MSR with OMP matches the time complexity of KroOMP (Caiafa & Cichocki, 2013), but reduces space complexity from $\mathcal{O}(N^I)$ to $\mathcal{O}(M^{I-1}N)$. For hierarchical sparsity, our MSR with HTP has time complexity $\mathcal{O}(MN^I)$ and space complexity $\mathcal{O}(M^{I-1}N)$, improving over HiHTP (Roth et al., 2020) with time and space complexities of $\mathcal{O}(M^2N^2)$ for $I = 2$. For Kronecker-supported sparsity, MSR with SBL lowers time complexity to $\mathcal{O}(MN^I)$ and space complexity to $\mathcal{O}(N^I)$ compared to AM- and SVD-KroSBL (He & Joseph, 2025a) with both complexities $\mathcal{O}(M^I N^I)$. The improvements are due to i) the exploitation of the Kronecker structure through tensor operation, reducing the dimensionality; and ii) leveraging the MMV structure from Lemma 1. We refer to Table 2 in Appendix E for a comprehensive comparison.

4 Unified Analysis for Structured Sparsity Models

We establish a unified RIP analysis via a generalized notion of RIP called the $(\boldsymbol{s}, \mathrm{N})$-RIP condition with $\boldsymbol{s} := (s_I, s_{I-1}, \cdots, s_1)$ and $\mathrm{N} := (N_I, N_{I-1}, \cdots, N_1)$ defined by the dimension of factor matrices in KCS. To this end, we introduce the generalized $(\boldsymbol{s}, \mathrm{N})$ sparsity model, tailored to the KCS problem, which reflects a hierarchical view where sparsity at each level affects recovery.

Sparsity 4 (Generalized sparsity)**.** *Consider KCS with $\boldsymbol{H}_i \in \mathbb{R}^{M_i \times N_i}$. A vector $\boldsymbol{x} \in \mathbb{R}^{\bar{N}}$ is $(\boldsymbol{s}, \mathrm{N})$ sparse if for tensor $\mathbf{X} \in \mathbb{R}^{N_1 \times \cdots \times N_I}$ reordered from $\boldsymbol{x}$ using $\mathrm{N} := (N_I, N_{I-1}, \cdots, N_1)$, the maximum number of nonzero rows of each of the column blocks of its jth mode unfolding $\boldsymbol{X}_{(j)}$ is s_j.*

Relation to other models: We relate the above model to the standard, hierarchical, Kronecker-supported, and block sparsity models. The standard sparsity model is not a special case of $(\boldsymbol{s}, \mathrm{N})$ sparsity, but the set of s sparse vectors is contained in a union of $(\boldsymbol{s}, \mathrm{N})$ sparse vectors.

Lemma 2. *Let set $\mathcal{S}$ contains all s standard sparse vectors in $\mathbb{R}^{\bar{N}}$, and $\mathcal{S}_{\boldsymbol{s}}$ contains all $(\boldsymbol{s}, \mathrm{N})$ sparse vectors in $\mathbb{R}^{\bar{N}}$ for a given $(\boldsymbol{s}, \mathrm{N})$. Then, $\mathcal{S} \subset \cup_{\boldsymbol{s} \in f_{\mathrm{N}}(s)} \mathcal{S}_{\boldsymbol{s}}$, where $f_{\mathrm{N}}(s) = \{\boldsymbol{s} : \sum_{i=1}^{I} s_i \leq s + (I-1),\ 1 \leq s_i \leq s\}$.*

Hierarchical sparsity is a special case of $(\boldsymbol{s}, \mathrm{N})$ sparsity when the hierarchical partition structure matches the dimensions of factor matrices in the Kronecker measurement matrix. If, additionally, all the column blocks of jth mode unfolding $\boldsymbol{X}_{(j)}$ share the same support regarding nonzero rows, then we arrive at the Kronecker-supported sparsity. Block sparsity can also be viewed as $(\boldsymbol{s}, \mathrm{N})$ sparsity with $I = 2$ when the block boundary matches the hierarchical partition structure.

We next define the $(\boldsymbol{s}, \mathrm{N})$-RIP condition for a Kronecker product matrix $\boldsymbol{H}$.

Definition 1 ($(\boldsymbol{s}, \mathrm{N})$-RIP)**.** *A Kronecker product matrix $\boldsymbol{H} = \otimes_{i=I}^{1} \boldsymbol{H}_i$ with $\boldsymbol{H}_i \in \mathbb{R}^{M_i \times N_i}$ satisfies $(\boldsymbol{s}, \mathrm{N})$-RIP if there exists $\delta \in (0, 1)$ such that for all $(\boldsymbol{s}, \mathrm{N})$ sparse $\boldsymbol{x} \in \mathbb{R}^{\bar{N}}$, it satisfies $(1-\delta)\|\boldsymbol{x}\|_2^2 \leq \|\boldsymbol{H}\boldsymbol{x}\|_2^2 \leq (1+\delta)\|\boldsymbol{x}\|_2^2$. The smallest feasible δ, denoted as $\delta_{(\boldsymbol{s},\mathrm{N})}(\boldsymbol{H})$, is the $(\boldsymbol{s}, \mathrm{N})$-RIC of $\boldsymbol{H}$.*

Under our models, $(\boldsymbol{s}, \mathrm{N})$-RIP is defined over the unions of subspaces, thus can be used to guarantee the success of recovery algorithms, such as iterative hard thresholding (IHT) and HTP (Blumensath, 2011). In general, such guarantees are established using the upper bound of the RICs. Therefore, we first derive the upper bound of $\delta_{(\boldsymbol{s},\mathrm{N})}(\boldsymbol{H})$, then discuss its implications for different sparsity models, and finally discuss the associated recovery algorithms and guarantees. Here, we denote the standard s-RIC of matrix $\boldsymbol{H}$ as $\delta_s(\boldsymbol{H})$.

Theorem 1. *The $(\boldsymbol{s}, \mathrm{N})$-RIC of Kronecker product dictionary $\boldsymbol{H} = \otimes_{i=I}^{1} \boldsymbol{H}_i$, i.e., $\delta_{(\boldsymbol{s},\mathrm{N})}(\boldsymbol{H})$, satisfies $\delta_{(\boldsymbol{s},\mathrm{N})}(\boldsymbol{H}) \leq \prod_{i=I}^{1}(1 + \delta_{s_i}(\boldsymbol{H}_i)) - 1$.*

The above result immediately applies to hierarchical and Kronecker-supported sparsity, as both are special cases of $(\boldsymbol{s}, \mathrm{N})$ sparsity. For Kronecker-supported sparsity, a tighter bound could be expected due to its additional joint sparsity structure arising from the shared support across the nonzero block. However, improving the RIC bound by exploiting this additional joint sparsity is difficult. As noted in Li & Petropulu (2013); Eldar & Mishali (2009), RIP analysis considers the worst-case performance and does not guarantee that MMV outperforms the SMV case. So, our bound shows no improvement, and deriving a stronger RIP-based condition for the MMV model is an open problem.

Theorem 1 can also be tailored to standard sparsity using Lemma 2.

Corollary 1. *Consider the Kronecker product $\boldsymbol{H} = \otimes_{i=I}^{1} \boldsymbol{H}_i$. For any s, the s-RIC of $\boldsymbol{H}$ satisfies $\delta_s(\boldsymbol{H}) \leq \max_{\boldsymbol{s} \in f_{\mathrm{N}}(s)} \delta_{(\boldsymbol{s},\mathrm{N})}(\boldsymbol{H}) \leq \max_{\boldsymbol{s} \in f_{\mathrm{N}}(s)} \prod_{i=1}^{I}(1 + \delta_{s_i}(\boldsymbol{H}_i)) - 1$.*

The s-RIC bound corroborates that only the sparsity level at different level of blocks explicitly affects the s-RIC of Kronecker-structured $\boldsymbol{H}$. Also, a known upper RIC bound is $\delta_s(\boldsymbol{H}) \leq \prod_{i=1}^{I}(1 + \delta_s(\boldsymbol{H}_i)) - 1$ (Duarte & Baraniuk, 2011a). Our bound slightly improves this bound:

$$\max_{\boldsymbol{s} \in f_{\mathrm{N}}(s)} \prod_{i=1}^{I}(1 + \delta_{s_i}(\boldsymbol{H}_i)) - 1 \leq \prod_{i=1}^{I}(1 + \delta_s(\boldsymbol{H}_i)) - 1,$$

because δ_s is a non-decreasing function of s (Foucart & Rauhut, 2013) and $s_i^* \leq s$ for all $i \in [I]$ and the equality cannot be achieved simultaneously.

Maximum sparsity level: Corollary 1 indicates that recovering s standard sparse vectors via KCS with $M_i < N_i$ is only guaranteed when $s < \min_i N_i$, as it is a worst-case analysis. When $s = \min_i N_i$ with $j = \arg\min_i N_i$, a worst-case scenario is $s_j = s = N_j$ and $s_i = 1$ for all $i \neq j$. Then, $\delta_{s_j} = \|\boldsymbol{H}_j^\top \boldsymbol{H}_j - \boldsymbol{I}_{N_j}\|_2 \geq 1$, making $\boldsymbol{H}_j$ is a non-injective map and recovery impossible. This also indicates that it is only possible to recover block-sparse vectors with block length smaller than $\min_i N_i$. However, recovery is still possible for $s \geq \min_i N_i$ in structured sparsity settings.

Measurement bounds for classical methods: We discuss the implications of Theorem 1 on measurement bounds for recovering $(\boldsymbol{s}, \mathrm{N})$-sparse vectors using classical iterative algorithms, namely

IHT and HTP. For both algorithms, at iteration k, the support is updated via thresholding operator $L_{\mathcal{S}}$ as $\mathcal{T}^{k+1} = L_{\mathcal{S}}\left(\boldsymbol{x}^k + \boldsymbol{H}^\top\left(\boldsymbol{y} - \boldsymbol{H}\boldsymbol{x}^k\right)\right)$. The thresholding operator depends on the sparsity model. For standard s sparse, $L_{\mathcal{S}}$ returns the support of the s largest entries of $\boldsymbol{x}$ in amplitude (Foucart & Rauhut, 2013). For $\boldsymbol{s}$ hierarchically sparse, it selects the top s_1 entries within each first-level block, then recursively picks top $s_2, \ldots, s_I$ blocks at higher levels based on the ℓ_2 norm, as in Roth et al. (2020). However, finding the thresholding operator $L_{\mathcal{S}}$ for $\boldsymbol{s}$ Kronecker-supported sparse vectors is NP-hard and not available in the literature. For example, when $I = 2$, it reduces to selecting rows and columns whose intersection maximizes the squared sum, equivalent to the NP-hard maximum weight biclique problem. A practical alternative is to first select the top s_I blocks at the Ith level by ℓ_2 norm, then recursively sum norms across matching indices at each lower level and select the top $s_{I-1}, \ldots, s_1$ blocks; this is the approach we use in simulations for comparison. Then, IHT applies a simple projection while HTP solves a least-squares problem on the support,

$$\boldsymbol{x}^{k+1} = \left(\boldsymbol{x}^k + \boldsymbol{H}^\top\left(\boldsymbol{y} - \boldsymbol{H}\boldsymbol{x}^k\right)\right)_{\mathcal{T}^{k+1}}, \tag{IHT}$$

$$\boldsymbol{x}^{k+1} = \arg\min_{\boldsymbol{x}\in\mathbb{R}^{\bar{N}}} \|\boldsymbol{y} - \boldsymbol{H}\boldsymbol{x}\|_2, \ \ \text{supp}(\boldsymbol{x}) \in \mathcal{T}^{k+1}, \tag{HTP}$$

where operator $(\cdot)_{\mathcal{T}^{k+1}}$ only preserves the entries within the set $\mathcal{T}^{k+1}$ and sets the others to zero.

We next discuss the implications for measurement bounds. It is known that for IHT and HTP to recover a vector from a union of subspaces, tailoring the thresholding operator $L_{\mathcal{S}}$ to the union and having an RIC below $1/\sqrt{3}$ over that union is sufficient to guarantee convergence to the ground truth (Foucart & Rauhut, 2013; Roth et al., 2020). So, our results shows that $\max_{\boldsymbol{s}\in f_{\mathrm{N}}(3s)} \delta_{(\boldsymbol{s},\mathrm{N})} < 1/\sqrt{3}$ (for s standard sparsity) and $\delta_{(3\boldsymbol{s},\mathrm{N})} < 1/\sqrt{3}$ (for $\boldsymbol{s}$ hierarchical sparsity) are sufficient for the success of IHT and HTP. However, it does not guarantee the recovery of the $\boldsymbol{s}$ Kronecker-supported sparse vectors as the thresholding operator is suboptimal.

To compare the measurement bound for KCS, we consider the simplest case with $I = 2$ and $s = \mathcal{O}(s_1 s_2)$ for $\boldsymbol{s} \in f_{\mathrm{N}}(s)$, and Gaussian factor matrices $\boldsymbol{H}_i$'s. For recovering s standard sparse vectors, our Corollary 1 implies that each $\boldsymbol{H}_i$ satisfies the s_i-RIP, requiring $M_i = \mathcal{O}(s_i \log N_i)$ (Foucart & Rauhut, 2013). So, the total measurement bound scales as $\bar{M} = \mathcal{O}(s_1 s_2 \log N_1 \log N_2)$ improving over the existing bound $\bar{M} = \mathcal{O}(s^2 \log N_1 \log N_2) = \mathcal{O}(s_1^2 s_2^2 \log N_1 \log N_2)$ (Duarte & Baraniuk, 2011a). In comparison, standard compressed sensing with *fully unstructured Gaussian matrix* requires only $\mathcal{O}(s_1 s_2 \log N_1 N_2)$ measurements, which is smaller due to greater flexibility and randomness in measurement. However, KCS exploits the multidimensional structure to reduce the computational complexity during recovery. For the recovery of $\boldsymbol{s}$ hierarchical sparse vectors, Corollary 1 suggests a measurement bound $\mathcal{O}(s_1 s_2 \log N_1 \log N_2)$, while a *fully unstructured Gaussian matrix* requires only $\mathcal{O}(s_1 s_2 \log N_1 + s_2 \log N_2)$ (Roth et al., 2020).

Measurement bounds for our MSR: We now establish recovery guarantees for MSR with IHT and HTP using the RICs of factor matrices.

Theorem 2. *Consider the sparse recovery problem, $\boldsymbol{y} = \left(\otimes_{i=I}^{1} \boldsymbol{H}_i\right)\boldsymbol{x} + \boldsymbol{n}$. Define tensors $\mathbf{X}$ and $\mathbf{N}$, which are reshaped from $\boldsymbol{x}$ and $\boldsymbol{n}$, respectively, using the dimensions of $\boldsymbol{H}_i$'s. If $\boldsymbol{x}$ is an s standard sparse vector and the factor matrices $\boldsymbol{H}_i$ for $i \in [I]$ satisfy $\delta_{3s_i}(\boldsymbol{H}_i) < 1/\sqrt{3}$ for $\forall \boldsymbol{s} \in f_{\mathrm{N}}(s)$, then the estimate $\hat{\boldsymbol{x}}$ of $\boldsymbol{x}$ using k-iteration IHT or HTP in Algorithm 1, satisfies*

$$\|\hat{\boldsymbol{x}} - \boldsymbol{x}\|_2 \le \max_{\boldsymbol{s}\in f_{\mathrm{N}}(s)} \sum_{n_2,\cdots,n_I} \left(\sum_{i=1}^{I} \prod_{j=1}^{i-1} \tau_j \alpha_i^k \left\| [\boldsymbol{U}_i]_{\mathrm{n_{i+1}}} \right\|_{\mathrm{F}} + \prod_{i=1}^{I} \tau_i \|\mathbf{N}\|_{\mathrm{F}} \right),$$

where $[\boldsymbol{U}_i]_{\mathrm{n_{i+1}}} = [\boldsymbol{X}_{(i)}]_{\mathrm{n_{i+1}}} \left(\otimes_{l=i-1}^{1} \boldsymbol{H}_l\right)^\top$, and if $\boldsymbol{x}$ is an $\boldsymbol{s}$ hierarchically sparse vector, and the factor matrices $\boldsymbol{H}_i$ for $i \in [I]$ satisfy $\delta_{3s_i}(\boldsymbol{H}_i) < 1/\sqrt{3}$, then the estimate $\hat{\boldsymbol{x}}$ of $\boldsymbol{x}$ using k-iteration IHT or HTP in Algorithm 1, satisfies

$$\|\hat{\boldsymbol{x}} - \boldsymbol{x}\|_2 \le \sum_{n_2,\cdots,n_I} \left(\sum_{i=1}^{I} \prod_{j=1}^{i-1} \tau_j \alpha_i^k \left\| [\boldsymbol{U}_i]_{\mathrm{n_{i+1}}} \right\|_{\mathrm{F}} + \prod_{i=1}^{I} \tau_i \|\mathbf{N}\|_{\mathrm{F}} \right),$$

and if $\boldsymbol{x}$ is an $\boldsymbol{s}$ Kronecker-supported sparse vector, there is

$$\|\hat{\boldsymbol{x}} - \boldsymbol{x}\|_2 \le \sum_{i=1}^{I} \prod_{j=1}^{i-1} \tau_j \alpha_i^k \|\boldsymbol{U}_i\|_{\mathrm{F}} + \prod_{i=1}^{I} \tau_i \|\mathbf{N}\|_{\mathrm{F}},$$

where $\boldsymbol{U}_i = \boldsymbol{X}_{(i)} \left(\boldsymbol{I}_{\prod_{l=I}^{i+1} N_l} \otimes \left(\otimes_{l=i-1}^{1} \boldsymbol{H}_l \right) \right)^\top$, *with* $\alpha_i < 1$, *and* τ_i *are*

$$\textit{MSIHT: } \alpha_i = \sqrt{3}\delta_{3s_i}(\boldsymbol{H}_i);\ \tau_i = (1-\alpha_i^k)\frac{\sqrt{3(1+\delta_{2s_i}(\boldsymbol{H}_i))}}{1-\alpha_i},\ \textit{and}$$

$$\textit{MSHTP: } \alpha_i = \sqrt{2\delta_{3s_i}^2(\boldsymbol{H}_i)/(1-\delta_{2s_i}^2(\boldsymbol{H}_i))};\ \tau_i = (1-\alpha_i^k)\frac{\sqrt{2(1-\delta_{2s_i}(\boldsymbol{H}_i))}+\sqrt{1+\delta_{s_i}(\boldsymbol{H}_i)}}{(1-\delta_{2s_i}(\boldsymbol{H}_i))\,(1-\alpha_i)}.$$

As the number of iterations $k \to \infty$, the error bound reduces to $\tau_1 \prod_{i=2}^{I} \tau_i N_i \|\mathbf{N}\|_{\mathrm{F}}$ for the standard and hierarchical sparsity, and $\prod_{i=1}^{I} \tau_i \|\mathbf{N}\|_{\mathrm{F}}$ for Kronecker-supported sparsity. So, MSIHT and MSHTP approach the true value within a constant factor of measurement noise power. Although factors $\tau_1 \prod_{i=2}^{I} \tau_i N_i$ and $\prod_{i=1}^{I} \tau_i$ suggest error propagation as the algorithm proceeds from $j = I$ till $j = 1$ and scale with the problem dimension, this amplification is not observed in practice (see Figure 3). The bound for $\boldsymbol{s}$ Kronecker-supported sparsity is tighter than that for the other two models because it solves a single MMV problem, resulting a collective error bound, instead of a looser bounds due to the sum of each individual MMV bound. While our MSR's measurement bound scales the same as classical methods due to a shared requirement on the s_i-RIP of $\boldsymbol{H}_i$'s, it can have a larger error from propagation, potentially requiring more iterations or $\boldsymbol{H}_i$'s with smaller s_i-RICs. However, a key advantage of MSR is that it provides recovery guarantees for the Kronecker-supported sparsity model, unlike classical IHT and HTP-based methods.

5 Numerical Evaluations

For numerical results, we combine MSR with MMV-SBL (Wipf & Rao, 2007), SIHT (Blanchard et al., 2014), SHTP (Blanchard et al., 2014), and SOMP (Tropp et al., 2006), and the resulting algorithms are referred to as MSSBL, MSIHT, MSHTP, and MSOMP, respectively. Our benchmark for the standard sparsity is KroOMP (Caiafa & Cichocki, 2013). Here, we omit computationally intensive SBL and OMP whose results are identical to KroOMP. For hierarchical sparsity, our benchmark is the state-of-the-art HiHTP (Roth et al., 2020). For Kronecker-structured support sparsity, we benchmark with the state-of-the-art AM- and SVD-KroSBL (He & Joseph, 2025a). Unlike the OMP/SBL-based algorithms, the IHT/HTP-based algorithms need the true sparsity level $\boldsymbol{s}$ as input.

For all three models, we set $M_i = M$, $N_i = N$, and $s_i = s$ for $i \in [I]$. For the s standard sparsity, we opt for $\boldsymbol{H} = \otimes_{i=I}^{1} \boldsymbol{H}_i$ with $I = 2$, $M = 64$, and $N = 80$. The entries of $\boldsymbol{H}_i$ and the nonzero entries of $\boldsymbol{x}$ are drawn independently from the standard normal distribution. We set $s = 15$, and the support is randomly drawn from a uniform distribution. For $\boldsymbol{s}$ hierarchically sparse vectors, we also opt for $I = 2$, $M = 64$, $N = 80$, and $s = 15$. Here, supports are generated by first selecting s blocks uniformly at random, then assigning support within each block uniformly. In the Kronecker-supported sparsity model, we opt for $I = 3$, $M = 15$, $N = 18$, and $s = 4$. The measurement noise is zero mean white Gaussian noise whose variance is determined by SNR (dB) $= 10 \log_{10} \mathbb{E}\{\|\boldsymbol{H}\boldsymbol{x}\|_2^2 / \|\boldsymbol{n}\|_2^2\}$ of $\{3, 5, \cdots, 23, 25\}$.

Our metrics are run time and the normalized squared error NSE $= \|\boldsymbol{x} - \hat{\boldsymbol{x}}\|_2^2 / \|\boldsymbol{x}\|_2^2$, where $\boldsymbol{x}$ is the ground truth and $\hat{\boldsymbol{x}}$ is the estimated vector. The results are shown in Figure 2 and Table 1, with the figure showing median and 25%/75% quartiles, and the table showing averages. The NSE for recovering an s standard sparse vector is shown in Figure 2a. Compared to KroOMP, MSOMP provides similar performance regarding NSE but needs one to three orders less run time, as in Table 1. MSSBL outperforms KroOMP in all SNR cases with one or two orders less run time. The NSE for hierarchical sparsity is shown in Figure 2b using only the HTP/IHT-based algorithms (full comparison in Appendix G). Our MSHTP/MSIHT offers similar performance as HTP and HiHTP, and IHT. However, MSHTP requires two orders less run time than HTP and one order less run time than HiHTP; and MSIHT requires two orders less run time than IHT. The NSE for Kronecker-supported sparsity is shown in Figure 2c. Our MSSBL consistently achieves a comparable NSE and is two or three orders faster than AM- and SVD-KroSBL. In summary, MSR variants achieve similar or better accuracy than existing methods while drastically reducing computation time.

Figure 3 shows how the NSE and run time (median with $25\%/75\%$ quartiles) of MSSBL, MSHTP, and MSIHT scale with the problem dimension, focusing on hierarchical sparsity. We choose $I = 3$ and SNR as 20dB and vary $N = \{50, 60, \cdots, 110\}$, so that the problem dimension $\bar{N} = N^I =$

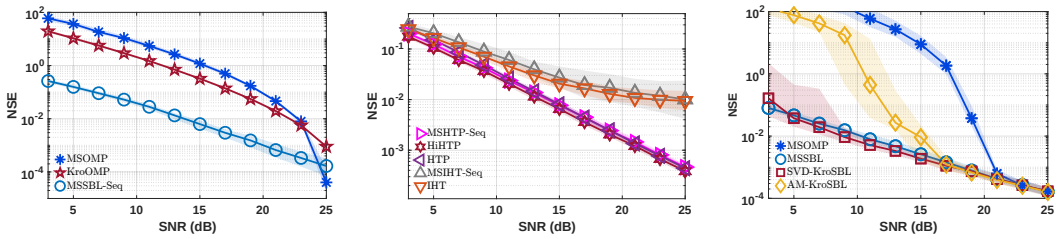

(a) Standard sparsity. (b) Hierarchical sparsity. (c) Kronecker-supported sparsity.

Figure 2: NSE as a function of SNR.

Table 1: Averaged runtime in seconds. **Bold**: the best result.

SNR	3 dB	7 dB	11 dB	15 dB	19 dB	23 dB
Recovery of s sparse vectors						
MSOMP-Seq	**0.4256**	**0.4119**	**0.3827**	0.3329	0.2204	**0.0568**
KroOMP (Caiafa & Cichocki, 2013)	130.5405	108.0526	76.6942	39.9844	11.5774	0.7525
MSSBL-Seq	1.8191	1.1016	0.5758	**0.2218**	**0.1417**	0.1141
Recovery of $\boldsymbol{s}$ hierarchically sparse vectors						
MSHTP-Seq	**0.0379**	**0.0305**	**0.0297**	**0.0247**	**0.0186**	**0.0168**
HiHTP (Roth et al., 2020)	0.6512	0.5493	0.5204	0.5444	0.4398	0.4574
HTP	2.2436	1.7170	1.3256	0.8450	0.8264	0.5311
MSIHT-Seq	0.0500	0.0510	0.0532	0.0509	0.0450	0.0434
IHT	8.2437	8.2412	8.2554	8.2917	8.2889	8.2789
Recovery of $\boldsymbol{s}$ Kronecker-supported sparse vectors						
MSOMP	**0.0042**	**0.0041**	**0.0040**	**0.0038**	**0.0026**	**0.0015**
MSSBL	0.0728	0.0587	0.0447	0.0279	0.0119	0.0051
SVD-KroSBL (He & Joseph, 2025a)	37.1233	26.9816	14.2405	8.6036	5.4067	4.0681
AM-KroSBL (He & Joseph, 2025a)	55.9532	63.4676	75.9727	74.5840	51.7089	34.1331

$125000, 216000, \cdots, 1331000$, where $M = \lceil (0.6\bar{N})^{1/I} \rceil$ and $s = \lceil (0.4\bar{N})^{1/I} \rceil$. As expected, parallel implementation is faster than sequential. MSSBL has the best NSE but is slower than MSIHT and MSHTP. The MSIHT is worse than MSHTP due to IHT's slow convergence (Foucart & Rauhut, 2013). Overall, our MSR efficiently handles large dimensional KCS problems.

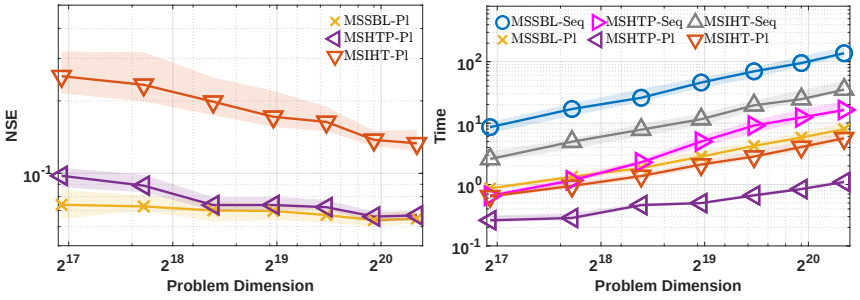

Figure 3: NSE and run time of MSR as functions of problem dimension $\bar{N}$.

6 Conclusion

We investigated the Kronecker compressed sensing problem for signals with multiple sparsity structures. We presented a novel hierarchical view, comprehending that each factor matrix in the Kronecker product dictionary senses the sparse signal at a different level, obeying a hierarchical structure. This insight led to a computationally efficient, multi-stage recovery framework that achieved performance comparable to state-of-the-art methods with one order or less run time. On the theoretical front, we unified the RIP analysis for Kronecker product matrices across various structured sparsity models, and also established the recovery guarantee for our multi-stage recovery algorithm. This hierarchical framework opens promising avenues for designing new algorithms to accommodate more structured patterns and provide efficient solutions to many applications.

7 Reproducibility Statement

All conditions required to reproduce the results are included in Section 5 and Appendix G. Our implementation and data for reproducing figures and tables are available as supplementary material.

References

Sebastian E Ament and Carla P Gomes. Sparse Bayesian learning via stepwise regression. In *Proceedings of the International Conference on Machine Learning*, pp. 264–274. PMLR, 2021.

Christian R Berger, Zhaohui Wang, Jianzhong Huang, and Shengli Zhou. Application of compressive sensing to sparse channel estimation. *IEEE Communications Magazine*, 48(11):164–174, 2010.

Jeffrey D Blanchard, Michael Cermak, David Hanle, and Yirong Jing. Greedy algorithms for joint sparse recovery. *IEEE Transactions on Signal Processing*, 62(7):1694–1704, Jan. 2014.

Thomas Blumensath. Sampling and reconstructing signals from a union of linear subspaces. *IEEE Transactions on Information Theory*, 57(7):4660–4671, July 2011.

Rémy Boyer and Martin Haardt. Noisy compressive sampling based on block-sparse tensors: Performance limits and beamforming techniques. *IEEE Transactions on Signal Processing*, 64(23): 6075–6088, 2016.

Cesar F Caiafa and Andrzej Cichocki. Block sparse representations of tensors using Kronecker bases. In *Proceedings of the IEEE International Conference on Acoustics, Speech, and Signal Processing*, pp. 2709–2712, Mar. 2012.

Cesar F Caiafa and Andrzej Cichocki. Computing sparse representations of multidimensional signals using Kronecker bases. *Neural Computation*, 25(1):186–220, Jan. 2013.

Wen-Che Chang and Yu T Su. Sparse Bayesian learning based tensor dictionary learning and signal recovery with application to MIMO channel estimation. *IEEE Journal of Selected Topics in Signal Processing*, 15(3):847–859, Apr. 2021.

Marco F Duarte and Richard G Baraniuk. Kronecker compressive sensing. *IEEE Transactions on Image Processing*, 21(2):494–504, Aug. 2011a.

Marco F Duarte and Richard G Baraniuk. Kronecker product matrices for compressive sensing. *Rice University, Houston, Technical Report*, Mar. 2011b. URL `http://www.ecs.umass.edu/mduarte/images/KroneckerCS-TREE1105.pdf`.

Marco F Duarte and Richard G Baraniuk. Kronecker product matrices for compressive sensing. In *Proceedings of the IEEE International Conference on Acoustics, Speech, and Signal Processing*, pp. 3650–3653, Mar. 2010.

Yonina C Eldar and Moshe Mishali. Robust recovery of signals from a structured union of subspaces. *IEEE Transactions on Information Theory*, 55(11):5302–5316, Oct. 2009.

Simon Foucart and Holger Rauhut. *A mathematical introduction to compressive sensing*. Birkhäuser Basel, 2013. ISBN 0817649476.

Shmuel Friedland, Qun Li, and Dan Schonfeld. Compressive sensing of sparse tensors. *IEEE Transactions on Image Processing*, 23(10):4438–4447, Oct. 2014.

Shmuel Friedland, Qun Li, Dan Schonfeld, and Edgar A Bernal. Two algorithms for compressed sensing of sparse tensors. In *Compressed Sensing and its Applications: MATHEON Workshop 2013*, pp. 259–281. Springer, 2015.

Yanbin He and Geethu Joseph. Structure-aware sparse Bayesian learning-based channel estimation for intelligent reflecting surface-aided MIMO. In *Proceedings of the IEEE International Conference on Acoustics, Speech, and Signal Processing*, pp. 1–5, Jun. 2023.

Yanbin He and Geethu Joseph. Bayesian algorithms for Kronecker-structured sparse vector recovery with application to IRS-MIMO channel estimation. *IEEE Transactions on Signal Processing*, 73: 142–157, 2025a.

Yanbin He and Geethu Joseph. Efficient off-grid Bayesian parameter estimation for Kronecker-structured signals. *IEEE Transactions on Signal Processing*, 73:2616–2630, 2025b.

Yanbin He and Geethu Joseph. A hierarchical view of structured sparsity in Kronecker compressive sensing. In *Proceedings of the European Signal Processing Conference*, pp. 1–5, Sept. 2025c.

Yanbin He and Geethu Joseph. Kronecker-structured sparse vector recovery with application to IRS-MIMO channel estimation. In *Proceedings of the IEEE International Conference on Acoustics, Speech, and Signal Processing*, pp. 1–5, Apr. 2025d.

The MathWorks Inc. Matlab version: 24.2.0.2923080 (r2024b), 2024.

Tamara G Kolda and Brett W Bader. Tensor decompositions and applications. *SIAM Review*, 51(3): 455–500, 2009.

Bo Li and Athina P Petropulu. Structured sampling of structured signals. In *Proceedings of the IEEE Global Conference on Signal and Information Processing*, pp. 1009–1012. IEEE, Feb. 2013.

Qun Li and Edgar A Bernal. An algorithm for parallel reconstruction of jointly sparse tensors with applications to hyperspectral imaging. In *Proceedings of the IEEE Conference on Computer Vision and Pattern Recognition Workshops*, pp. 24–31, 2017.

Yair Rivenson and Adrian Stern. Compressed imaging with a separable sensing operator. *IEEE Signal Processing Letters*, 16(6):449–452, 2009.

Ingo Roth, Axel Flinth, Richard Kueng, Jens Eisert, and Gerhard Wunder. Hierarchical restricted isometry property for Kronecker product measurements. In *Proceedings of the Annual Allerton Conference on Communication, Control, and Computing*, pp. 632–638. IEEE, 2018.

Ingo Roth, Martin Kliesch, Axel Flinth, Gerhard Wunder, and Jens Eisert. Reliable recovery of hierarchically sparse signals for Gaussian and Kronecker product measurements. *IEEE Transactions on Signal Processing*, 68:4002–4016, June 2020.

Luning Sun, Daniel Huang, Hao Sun, and Jian-Xun Wang. Bayesian spline learning for equation discovery of nonlinear dynamics with quantified uncertainty. *Proceedings of Advances in Neural Information Processing Systems*, 35:6927–6940, 2022.

Joel A Tropp, Anna C Gilbert, and Martin J Strauss. Algorithms for simultaneous sparse approximation. Part I: Greedy pursuit. *Signal Processing*, 86(3):572–588, 2006.

N. Vervliet, O. Debals, L. Sorber, M. Van Barel, and L. De Lathauwer. Tensorlab 3.0, Mar. 2016. URL `https://www.tensorlab.net`. Available online.

David P Wipf and Bhaskar D Rao. Sparse Bayesian learning for basis selection. *IEEE Transactions on Signal Processing*, 52(8):2153–2164, Aug. 2004.

David P Wipf and Bhaskar D Rao. An empirical Bayesian strategy for solving the simultaneous sparse approximation problem. *IEEE Transactions on Signal Processing*, 55(7):3704–3716, June 2007.

Gerhard Wunder, Ingo Roth, Rick Fritschek, and Jens Eisert. Hihtp: A custom-tailored hierarchical sparse detector for massive MTC. In *Proceedings of the Asilomar Conference on Signals, Systems, and Computers*, pp. 1929–1934. IEEE, 2017.

Zhenyu Xiao, Songqi Cao, Lipeng Zhu, Yanming Liu, Boyu Ning, Xiang-Gen Xia, and Rui Zhang. Channel estimation for movable antenna communication systems: A framework based on compressed sensing. *IEEE Transactions on Wireless Communications*, 23(9):11814–11830, 2024.

Xiaowen Xu, Shun Zhang, Feifei Gao, and Jiangzhou Wang. Sparse Bayesian learning based channel extrapolation for RIS assisted MIMO-OFDM. *IEEE Transactions on Communications*, 70(8): 5498–5513, Aug. 2022.

Ye Yuan, Xiuchuan Tang, Wei Zhou, Wei Pan, Xiuting Li, Hai-Tao Zhang, Han Ding, and Jorge Goncalves. Data driven discovery of cyber physical systems. *Nature Communications*, 10(1): 4894, 2019.

Rongqiang Zhao, Qiang Wang, Jun Fu, and Luquan Ren. Exploiting block-sparsity for hyperspectral Kronecker compressive sensing: A tensor-based Bayesian method. *IEEE Transactions on Image Processing*, 29:1654–1668, Oct. 2019.

A PROOF OF LEMMA 1

Before diving into the details, we explain the notation in the Figure 4. The arrow in Figure 4 means the corresponding index runs through all its values in ascending order. For example, an arrow with n_j means $n_j = 1, 2, \ldots, N_j$. For two indices n_p and n_q with $p \neq q$, the ordering is hierarchical: if $p > q$, then n_p is treated as the outer index, while n_q is the inner index. Consequently, for each fixed value of n_p in $1, \ldots, N_p$, the index n_q spans its entire range repeatedly. Hence, unfolding a tensor along its jth dimension is reshaping the tensor to a matrix where rows are indexed by $n_j = 1, 2, \ldots, N_j$, while columns are indexed by the remaining indices arranged according to this hierarchical ordering.

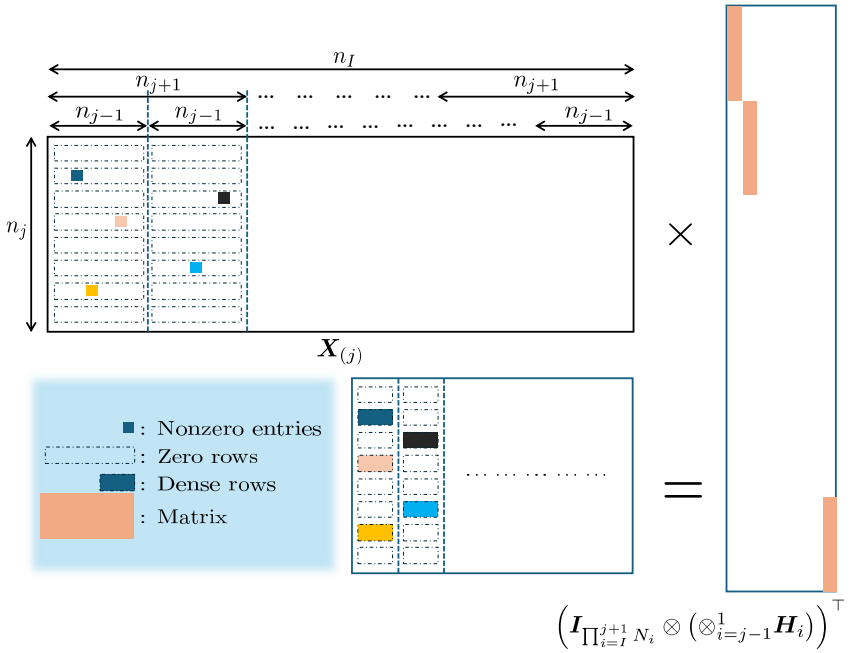

Figure 4: An illustrating of the proof of Lemma 1.

The proof proceeds in two parts: first, establishing the column block structure, and second, analyzing the sparsity of each block.

For the first step, we observe that matrix $\left(\boldsymbol{I}_{\prod_{i=I}^{j+1} N_i} \otimes \left(\otimes_{i=j-1}^{1} \boldsymbol{H}_i\right)\right)^\top$ is a *block-diagonal matrix*. It has $\prod_{i=I}^{j+1} N_i$ identical diagonal blocks, each equal to $\left(\otimes_{i=j-1}^{1} \boldsymbol{H}_i\right)^\top$. To match this structure, we partition the columns of the unfolded matrix $\mathbf{X}_{(j)}$ into $\prod_{i=I}^{j+1} N_i$ column blocks. The standard column ordering in tensor unfolding places elements with higher-level indices $(n_{j+1}, \ldots, n_I)$ further apart. Consequently, we can partition $\mathbf{X}_{(j)}$ into $\prod_{i=j+1}^{I} N_i$ column blocks, where each block corresponds to a unique *encapsulation* $\mathrm{n_{j+1}} = (n_{j+1}, \ldots, n_I)$ as

$$\boldsymbol{X}_{(j)} = \begin{bmatrix} \boldsymbol{X}_{(j),(1,\ldots,1)} & \cdots & \boldsymbol{X}_{(j),(N_{j+1},\ldots,N_I)} \end{bmatrix}.$$

Since $\left(\boldsymbol{I}_{\prod_{i=I}^{j+1} N_i} \otimes \left(\otimes_{i=j-1}^{1} \boldsymbol{H}_i\right)\right)^\top$ is block-diagonal, the multiplication with $\boldsymbol{X}_{(j)}$ decouples and operates on each of these blocks independently,

$$\boldsymbol{X}_{(j)} \left(\boldsymbol{I}_{\prod_{i=I}^{j+1} N_i} \otimes \left(\otimes_{i=j-1}^{1} \boldsymbol{H}_i\right)\right)^\top = \begin{bmatrix} \boldsymbol{X}_{(j),(1,\ldots,1)} \left(\otimes_{i=j-1}^{1} \boldsymbol{H}_i\right)^\top & \cdots & \boldsymbol{X}_{(j),(N_{j+1},\ldots,N_I)} \left(\otimes_{i=j-1}^{1} \boldsymbol{H}_i\right)^\top \end{bmatrix}.$$

This confirms that the resulting matrix is also composed of $\prod_{i=j+1}^{I} N_i$ column blocks, each indexed by $\mathrm{n_{j+1}}$ and given by $\boldsymbol{X}_{(j),\mathrm{n_{j+1}}} \left(\otimes_{i=j-1}^{1} \boldsymbol{H}_i\right)^\top$.

For the second step, consider a column block indexed by a fixed $\mathrm{n_{j+1}}$, i.e., $\boldsymbol{X}_{(j),\mathrm{n_{j+1}}} \left(\otimes_{i=j-1}^{1} \boldsymbol{H}_i\right)^\top$. The rows of this block are indexed by $n_j \in [N_j]$. The kth row of $\boldsymbol{X}_{(j),\mathrm{n_{j+1}}} \left(\otimes_{i=j-1}^{1} \boldsymbol{H}_i\right)^\top$ will be nonzero *if and only if* the kth row of $\boldsymbol{X}_{(j),\mathrm{n_{j+1}}}$ contains nonzeros due to the full row rankness. Moreover, the kth row of $\boldsymbol{X}_{(j),\mathrm{n_{j+1}}}$ is the hierarchical block $\boldsymbol{x}_{\mathrm{n_j}}$ where the encapsulation is $\mathrm{n_j} = (k, n_{j+1}, \ldots, n_I)$. This equivalence follows because the indices of the entries in the kth row of $\boldsymbol{X}_{(j),\mathrm{n_{j+1}}}$ align exactly with those of the hierarchical block $\boldsymbol{x}_{\mathrm{n_j}}$ with $\mathrm{n_j} = (k, n_{j+1}, \ldots, n_I)$. Hence, the kth row of $\boldsymbol{X}_{(j),\mathrm{n_{j+1}}}$ and the hierarchical block $\boldsymbol{x}_{\mathrm{n_j}}$ with $\mathrm{n_j} = (k, n_{j+1}, \ldots, n_I)$ contain identical entries with identical order. Thus, the number of non-zero rows in $\boldsymbol{X}_{(j),\mathrm{n_{j+1}}} \left(\otimes_{i=j-1}^{1} \boldsymbol{H}_i\right)^\top$ is the number of hierarchical blocks $\{\boldsymbol{x}_{\mathrm{n_j}}\}$ (within the parent block defined by $\mathrm{n_{j+1}}$) that contain at least one non-zero element, which concludes the proof.

B Proof of Lemma 2

Let $\boldsymbol{x}$ be an s sparse vector. We denote k_j as the total number of nonzero blocks within all jth-level blocks of $\boldsymbol{x}$. Clearly, $k_1 = s$ and $k_{I+1} = 1$. Then, each nonzero block in the $j+1$th level can have at most $k_j - (k_{j+1} - 1)$ number of nonzero jth level blocks. This occurs in the most unbalanced case, where $k_{j+1} - 1$ blocks have only one nonzero jth level block while the remaining block has $k_j - (k_{j+1} - 1)$ nonzero jth level blocks. This observation leads to the upper bound for the sparsity level, $s_j \leq k_j - (k_{j+1} - 1)$, which yields $\sum_{i=1}^{I} s_i \leq s + (I - 1)$. So, any s sparse vector $\boldsymbol{x} \in \cup_{\boldsymbol{s} \in f_{\mathrm{N}}(s)} \mathcal{S}_{\boldsymbol{s}}$.

C Proof of Theorem 1

For any $\boldsymbol{x}$, we note that Equation 1 bounds $\|\boldsymbol{H}\boldsymbol{x}\|_2^2$. Following the hierarchical view, we note

$$\|\boldsymbol{H}\boldsymbol{x}\|_2^2 = \|\mathbf{X} \times_1 \boldsymbol{H}_1 \cdots \times_I \boldsymbol{H}_I\|_{\mathrm{F}}^2 = \|\boldsymbol{H}_I \boldsymbol{X}_{(I)} \left(\otimes_{i=I-1}^{1} \boldsymbol{H}_i\right)^\top\|_{\mathrm{F}}^2.$$

Using the RIC of $\boldsymbol{H}_I$, we have

$$(1 - \delta_{s_I}) \|\boldsymbol{X}_{(I)} \left(\otimes_{i=I-1}^{1} \boldsymbol{H}_i\right)^\top\|_{\mathrm{F}}^2 \leq \|\boldsymbol{H}\boldsymbol{x}\|_2^2 \leq (1 + \delta_{s_I}) \|\boldsymbol{X}_{(I)} \left(\otimes_{i=I-1}^{1} \boldsymbol{H}_i\right)^\top\|_{\mathrm{F}}^2.$$

We also note that $\|\boldsymbol{X}_{(I)} \left(\otimes_{i=I-1}^{1} \boldsymbol{H}_i\right)^\top\|_{\mathrm{F}}^2 = \|\boldsymbol{H}_{I-1} \boldsymbol{X}_{(I-1)} \left(\boldsymbol{I}_{N_I} \otimes \left(\otimes_{i=I-2}^{1} \boldsymbol{H}_i\right)\right)^\top\|_{\mathrm{F}}^2$ due to the tensor folding and unfolding. Therefore, using RIC of $\boldsymbol{H}_{I-1}$, we arrive at

$$\begin{aligned}(1 - \delta_{s_I})(1 - \delta_{s_{I-1}}) \|\boldsymbol{X}_{(I-1)} \left(\boldsymbol{I}_{N_I} \otimes \left(\otimes_{i=I-2}^{1} \boldsymbol{H}_i\right)\right)^\top\|_{\mathrm{F}}^2 \\ \leq \|\boldsymbol{H}\boldsymbol{x}\|_2^2 \leq (1 + \delta_{s_I})(1 + \delta_{s_{I-1}}) \|\boldsymbol{X}_{(I)} \left(\otimes_{i=I-1}^{1} \boldsymbol{H}_i\right)^\top\|_{\mathrm{F}}^2\end{aligned}$$

Repeating these steps recursively following the analysis in hierarchical view, we obtain

$$\prod_{i=1}^{I} (1 - \delta_{s_i}) \|\boldsymbol{X}_{(1)} \left(\otimes_{i=I-1}^{1} \boldsymbol{I}_{N_i}\right)^\top\|_{\mathrm{F}}^2 \leq \|\boldsymbol{H}\boldsymbol{x}\|_2^2 \leq \prod_{i=1}^{I} (1 + \delta_{s_i}) \|\boldsymbol{X}_{(1)} \left(\otimes_{i=I-1}^{1} \boldsymbol{I}_{N_i}\right)^\top\|_{\mathrm{F}}^2.$$

Since $\boldsymbol{X}_{(1)} \left(\otimes_{i=I-1}^{1} \boldsymbol{I}_{N_i}\right)^\top = \boldsymbol{X}_{(1)}$ and $\|\boldsymbol{X}_{(1)}\|_{\mathrm{F}}^2 = \|\boldsymbol{x}\|_2^2$,

$$\prod_{i=1}^{I} (1 - \delta_{s_i}) \|\boldsymbol{x}\|_2^2 \leq \|\boldsymbol{H}\boldsymbol{x}\|_2^2 \leq \prod_{i=1}^{I} (1 + \delta_{s_i}) \|\boldsymbol{x}\|_2^2.$$

Hence, we derive

$$\delta_{(\boldsymbol{s},\mathrm{N})}(\boldsymbol{H}) \leq \max\{1 - \prod_{i=1}^{I} (1 - \delta_{s_i}), \prod_{i=1}^{I} (1 + \delta_{s_i}) - 1\} = \prod_{i=1}^{I} (1 + \delta_{s_i}) - 1,$$

which completes the proof.

D Complete Results on the Number of Measurements

In this section, we present the measurement bounds for unstructured $\boldsymbol{H}$ with different sparsity patterns. Let $\boldsymbol{H} \in \mathbb{R}^{\bar{M}\times\bar{N}}$ has independent and identically distributed standard Gaussian. For

$$\bar{M} = \mathcal{O}\left(s\ln(\frac{e\bar{N}}{s})\right)$$

where c is a positive constant, s sparse vectors can be recovered from the measurement of $\boldsymbol{H}$ with high probability (Foucart & Rauhut, 2013). Also, if

$$\bar{M} = \mathcal{O}\left(\sum_{i=1}^{I}\prod_{j=i}^{I} s_j \ln(\frac{eN_i}{s_i}) + \prod_{i=1}^{I} s_i\right),$$

$\boldsymbol{s}$ hierarchical sparse vectors can be recovered from the measurement of $\boldsymbol{H}$ with high probability (Roth et al., 2020).

E Complexity Comparison

We comprehensively analyze the complexity of our MSR algorithm to demonstrate the benefit of exploiting the Kronecker structure of $\boldsymbol{H}$ via the hierarchical view. We consider MSR combined with MMV-SBL (Wipf & Rao, 2007), SIHT (Blanchard et al., 2014), SHTP (Blanchard et al., 2014), and SOMP (Tropp et al., 2006) as sparse recovery algorithms, referred to as MSSBL, MSIHT, MSHTP, and MSOMP, respectively. We also use `Seq` and `Pl` to represent the *sequential* and *parallel* implementation of Equation 5. Assume M_i's are $\mathcal{O}(M)$, N_i's are $\mathcal{O}(N)$ for $i \in [I]$, and $I < M < N$. We compare the time and space complexity of our algorithms with other state-of-the-art algorithms. For the recovery of s sparse vectors, we include SBL (Wipf & Rao, 2004), OMP, and KroOMP (Caiafa & Cichocki, 2013) as benchmarks. For the recovery of $\boldsymbol{s}$ hierarchically sparse vectors, HiHTP (Roth et al., 2020), IHT, and HTP are used as benchmarks. We note that only the exact implementation of HiHTP for $I = 2$ is given in (Roth et al., 2020). Regarding recovering $\boldsymbol{s}$ Kronecker-supported sparse vectors, we consider AM- and SVD-KroSBL (He & Joseph, 2025a) for benchmarking.

For the recovery of s standard sparse vectors, our MSSBL and MSOMP substantially reduce both the time and space complexity compared to their traditional counterparts. In terms of time complexity, our MSSBL ($\mathcal{O}(M^2N^I)$ for `Seq` and $\mathcal{O}(M^IN)$ for `Pl`) is superior than SBL ($\mathcal{O}(M^{2I}N^I)$), while the time complexity of MSOMP ($\mathcal{O}(MN^I)$ for `Seq` and $\mathcal{O}(M^IN)$ for `Pl`) is also lower than OMP with $\mathcal{O}(M^IN^I)$. Moreover, both MSSBL and MSOMP avoid $\mathcal{O}(MN)^I$ in space complexity and have $\mathcal{O}(M^{I-1}N)$ for `Seq` and $\mathcal{O}(MN^I)$ for `Pl`. Compared to KroOMP with time complexity $\mathcal{O}(MN^I)$ and space complexity $\mathcal{O}(N^I)$, MSOMP-`Seq` achieves the same time complexity but with a much lower space complexity $\mathcal{O}(M^{I-1}N)$. Alternatively, we can achieve a much lower time complexity $\mathcal{O}(M^IN)$ by parallel implementation, at the cost of a slightly higher space complexity of $\mathcal{O}(MN^I)$.

The computational gains are particularly significant regarding structured sparsity. For both hierarchically sparse and Kronecker-supported sparse vectors, classical methods like IHT and HTP exhibit a time and space complexity of $\mathcal{O}(M^IN^I)$. Our MSIHT-`Seq`, MSHTP-`Seq`, and MSSBL-`Seq` have time complexity $\mathcal{O}(MN^I)$, $\mathcal{O}(MN^I)$, and $\mathcal{O}(M^2N^I)$, respectively, and $\mathcal{O}(M^{I-1}N)$ for space complexity. Compared to HiHTP, our MSSBL-`Seq` has the same time complexity $\mathcal{O}(M^2N^2)$ while MSSBL-`Pl` has a lower space complexity ($\mathcal{O}(MN^2)$ compared to $\mathcal{O}(M^2N^2)$ of HiHTP.

Similarly, for Kronecker-supported sparse recovery, when compared to AM-KroSBL and SVD-KroSBL, MSSBL algorithm demonstrates lower time complexity from $\mathcal{O}(M^IN^I)$ to $\mathcal{O}(MN^I)$ and space complexity from $\mathcal{O}(M^IN^I)$ to $\mathcal{O}(N^I)$. MSIHT and MSHTP exhibit the same or even lower time and space complexity than MSSBL, hence lower than AM-KroSBL and SVD-KroSBL, demonstrating the superiority of our multi-stage framework. We list all the time and space complexity of the algorithms in Table 2. We use R_{EM}, R_{OMP}, R_{HTP}, R_{IHT}, and R_{AM} to denote the number of EM, OMP, HTP, IHT, and AM iterations. All these values can vary for different algorithms and experiment settings.

Table 2: Complexity of different algorithms in different sparse recovery problems.

Method	Time Complexity	Space Complexity
Recovery of s sparse vectors		
MSSBL-`Seq`	$\mathcal{O}\big(R_{\mathrm{EM}}(M^2N^I + MN^I)\big)$	$\mathcal{O}(M^{I-1}N)$
MSSBL-`Pl`	$\mathcal{O}\big(R_{\mathrm{EM}}(IM^2N + M^IN)\big)$	$\mathcal{O}(MN^I)$
MSOMP-`Seq`	$\mathcal{O}\big(R_{\mathrm{OMP}}MN^I + R^3_{\mathrm{OMP}}N^{I-1} + R^2_{\mathrm{OMP}}MN^{I-1}\big)$	$\mathcal{O}(M^{I-1}N)$
MSOMP-`Pl`	$\mathcal{O}\big(R_{\mathrm{OMP}}M^IN + R^2_{\mathrm{OMP}}M^I + R^3_{\mathrm{OMP}}M^{I-1}\big)$	$\mathcal{O}(MN^I)$
KroOMP	$\mathcal{O}\big(R_{\mathrm{OMP}}MN^I + R^2_{\mathrm{OMP}}M^I + R^2_{\mathrm{OMP}}MN + R^3_{\mathrm{OMP}}\big)$	$\mathcal{O}(N^I)$
SBL	$\mathcal{O}\big(R_{\mathrm{EM}}M^{2I}N^I\big)$	$\mathcal{O}((MN)^I)$
OMP	$\mathcal{O}\big(R_{\mathrm{OMP}}(MN)^I + R^3_{\mathrm{OMP}} + R^2_{\mathrm{OMP}}M^I\big)$	$\mathcal{O}((MN)^I)$
Recovery of $\boldsymbol{s}$ hierarchically sparse vectors		
MSSBL-`Seq`	$\mathcal{O}\big(R_{\mathrm{EM}}(M^2N^I + MN^I)\big)$	$\mathcal{O}(M^{I-1}N)$
MSSBL-`Pl`	$\mathcal{O}\big(R_{\mathrm{EM}}(IM^2N + M^IN)\big)$	$\mathcal{O}(MN^I)$
MSHTP-`Seq`	$\mathcal{O}\big(R_{\mathrm{HTP}}(MN^I + \max_i s_i^2MN^{I-1})\big)$	$\mathcal{O}(M^{I-1}N)$
MSIHT-`Seq`	$\mathcal{O}\big(R_{\mathrm{IHT}}MN^I\big)$	$\mathcal{O}(M^{I-1}N)$
HiHTP Roth et al. (2020) ($I=2$)	$\mathcal{O}\big(R_{\mathrm{HTP}}((s_1s_2)^2M^2 + (MN)^2)\big)$	$\mathcal{O}((MN)^2)$
IHT	$\mathcal{O}\big(R_{\mathrm{IHT}}(MN)^I\big)$	$\mathcal{O}((MN)^I)$
HTP	$\mathcal{O}\big(R_{\mathrm{HTP}}((MN)^I + (\prod_{i=1}^I s_i)^2M^I)\big)$	$\mathcal{O}((MN)^I)$
Recovery of $\boldsymbol{s}$ Kronecker-supported sparse vectors		
MSSBL	$\mathcal{O}\big(R_{\mathrm{EM}}(IM^2N + MN^I)\big)$	$\mathcal{O}(N^I)$
MSIHT	$\mathcal{O}\big(R_{\mathrm{IHT}}MN^I\big)$	$\mathcal{O}(N^I)$
MSHTP	$\mathcal{O}\big(R_{\mathrm{HTP}}MN^I + R_{\mathrm{HTP}}M\sum_{i=1}^I s_i^2)\big)$	$\mathcal{O}(N^I)$
MSOMP	$\mathcal{O}\big(R^3_{\mathrm{OMP}}N^{I-1} + R^2_{\mathrm{OMP}}MN^{I-1} + R_{\mathrm{OMP}}MN^I\big)$	$\mathcal{O}(N^I)$
AM-KroSBL He & Joseph (2025a)	$\mathcal{O}\big(R_{\mathrm{EM}}(R_{\mathrm{AM}}IN^I + (MN)^I)\big)$	$\mathcal{O}((MN)^I)$
SVD-KroSBL He & Joseph (2025a)	$\mathcal{O}\big(R_{\mathrm{EM}}(N^{I+1} + (MN)^I)\big)$	$\mathcal{O}((MN)^I)$
IHT	$\mathcal{O}\big(R_{\mathrm{IHT}}(MN)^I\big)$	$\mathcal{O}((MN)^I)$
HTP	$\mathcal{O}\big(R_{\mathrm{HTP}}((MN)^I + (\prod_{i=1}^I s_i)^2M^I)\big)$	$\mathcal{O}((MN)^I)$

F Proof of Theorem 2

Before the proof of Theorem 2, we introduce four aiding lemmas.

Lemma 3. *(Foucart & Rauhut, 2013, Lemma 6.16) Given a vector $\boldsymbol{v} \in \mathbb{R}^N$ and an index set $\mathcal{T} \subset [N]$, there is*

$$\|((\boldsymbol{I}_N - \boldsymbol{H}^\top\boldsymbol{H})\boldsymbol{v})_\mathcal{T}\|_2 \le \delta_t\|\boldsymbol{v}\|_2,$$

if the cardinality of the union of $\mathcal{T}$ and the support set of $\boldsymbol{v}$ is not exceeding t.

Lemma 4. *(Foucart & Rauhut, 2013, Lemma 6.20) Given vector $\boldsymbol{n} \in \mathbb{R}^N$ and set $\mathcal{T} \subset [N]$ with cardinality not exceeding s, then*

$$\|(\boldsymbol{H}^\top\boldsymbol{n})_\mathcal{T}\|_2 \le \sqrt{1+\delta_s}\|\boldsymbol{n}\|_2.$$

Lemma 5. *For sparse matrix $\boldsymbol{X}$ with row support $\mathcal{T}$ with $\mathrm{card}(\mathcal{T}) \le s$, and $\boldsymbol{N} \in \mathbb{R}^{M\times N}$, the sequence $\{\boldsymbol{X}^k\}$ defined by SIHT or SHTP for solving an MMV problem $\boldsymbol{Y} = \boldsymbol{H}\boldsymbol{X} + \boldsymbol{N}$ with $\boldsymbol{X}^0 = \boldsymbol{0}$, satisfies for any $k \ge 0$,*

$$\|\boldsymbol{X}^k - \boldsymbol{X}\|_\mathrm{F} \le \alpha^k\|\boldsymbol{X}\|_\mathrm{F} + \tau\|\boldsymbol{N}\|_\mathrm{F},$$

where

$$\textit{for SIHT: } \alpha = \sqrt{3}\delta_{3s}, \tau = \sqrt{3(1+\delta_{2s})}\frac{1-\alpha^k}{1-\alpha}, \textit{ and}$$

$$\textit{for SHTP: } \alpha = \sqrt{\frac{2\delta_{3s}^2}{1-\delta_{2s}^2}}, \tau = \frac{(\sqrt{2(1-\delta_{2s})}+\sqrt{1+\delta_s})(1-\alpha^k)}{(1-\delta_{2s})(1-\alpha)}.$$

Proof. The proof closely follows the technique in Foucart & Rauhut (2013, Theorem 6.18) and Blanchard et al. (2014). Here, we extend the SMV case in Foucart & Rauhut (2013, Theorem 6.18) to the MMV case. In the MMV case, the thresholding operator retains the rows of $\boldsymbol{X}^k + \boldsymbol{H}^\top\left(\boldsymbol{Y} - \boldsymbol{H}\boldsymbol{X}^k\right)$ with the s largest row ℓ_2 norms, and then we have

$$\|\left(\boldsymbol{X}^k + \boldsymbol{H}^\top\left(\boldsymbol{Y} - \boldsymbol{H}\boldsymbol{X}^k\right)\right)_\mathcal{T}\|_\mathrm{F}^2 \le \|\left(\boldsymbol{X}^k + \boldsymbol{H}^\top\left(\boldsymbol{Y} - \boldsymbol{H}\boldsymbol{X}^k\right)\right)_{\mathcal{T}^{k+1}}\|_\mathrm{F}^2.$$

Removing the common rows from both sides, we arrive at

$$\| \left(\boldsymbol{X}^k + \boldsymbol{H}^\top \left(\boldsymbol{Y} - \boldsymbol{H}\boldsymbol{X}^k\right)\right)_{\mathcal{T}\setminus\mathcal{T}^{k+1}} \|_{\mathrm{F}}^2 \leq \| \left(\boldsymbol{X}^k + \boldsymbol{H}^\top \left(\boldsymbol{Y} - \boldsymbol{H}\boldsymbol{X}^k\right)\right)_{\mathcal{T}^{k+1}\setminus\mathcal{T}} \|_{\mathrm{F}}^2.$$

IHT proceeds with $\boldsymbol{X}^{k+1} = \left(\boldsymbol{X}^k + \boldsymbol{H}^\top \left(\boldsymbol{Y} - \boldsymbol{H}\boldsymbol{X}^k\right)\right)_{\mathcal{T}^{k+1}}$. Since $(\boldsymbol{X}^{k+1})_{\mathcal{T}\setminus\mathcal{T}^{k+1}} = \boldsymbol{0}$ and $(\boldsymbol{X})_{\mathcal{T}^{k+1}\setminus\mathcal{T}} = \boldsymbol{0}$, we get

$$\begin{aligned}
&\| \left(\boldsymbol{X} - \boldsymbol{X}^{k+1} + \boldsymbol{X}^k - \boldsymbol{X} + \boldsymbol{H}^\top \left(\boldsymbol{Y} - \boldsymbol{H}\boldsymbol{X}^k\right)\right)_{\mathcal{T}\setminus\mathcal{T}^{k+1}} \|_{\mathrm{F}} \\
&\qquad \leq \| \left(\boldsymbol{X}^k - \boldsymbol{X} + \boldsymbol{H}^\top \left(\boldsymbol{Y} - \boldsymbol{H}\boldsymbol{X}^k\right)\right)_{\mathcal{T}^{k+1}\setminus\mathcal{T}} \|_{\mathrm{F}}.
\end{aligned}$$

Applying reverse triangle inequality to the left-hand side and rearranging, we arrive at

$$\begin{aligned}
\| \left(\boldsymbol{X} - \boldsymbol{X}^{k+1}\right)_{\mathcal{T}\setminus\mathcal{T}^{k+1}} \|_{\mathrm{F}} &\leq \| \left(\boldsymbol{X}^k - \boldsymbol{X} + \boldsymbol{H}^\top \left(\boldsymbol{Y} - \boldsymbol{H}\boldsymbol{X}^k\right)\right)_{\mathcal{T}^{k+1}\setminus\mathcal{T}} \|_{\mathrm{F}} \\
&\quad + \| \left(\boldsymbol{X}^k - \boldsymbol{X} + \boldsymbol{H}^\top \left(\boldsymbol{Y} - \boldsymbol{H}\boldsymbol{X}^k\right)\right)_{\mathcal{T}\setminus\mathcal{T}^{k+1}} \|_{\mathrm{F}} \\
&\leq \sqrt{2} \| \left(\boldsymbol{X}^k - \boldsymbol{X} + \boldsymbol{H}^\top \left(\boldsymbol{Y} - \boldsymbol{H}\boldsymbol{X}^k\right)\right)_{\mathcal{T}\Delta\mathcal{T}^{k+1}} \|_{\mathrm{F}},
\end{aligned}$$

where $\mathcal{T}\Delta\mathcal{T}^{k+1} = (\mathcal{T} \setminus \mathcal{T}^{k+1}) \cup (\mathcal{T}^{k+1} \setminus \mathcal{T})$ denoting the symmetric difference of the sets $\mathcal{T}$ and $\mathcal{T}^{k+1}$. Therefore, we obtain the error in the kth iteration as

$$\begin{aligned}
\|\boldsymbol{X}^{k+1} - \boldsymbol{X}\|_{\mathrm{F}}^2 &= \| \left(\boldsymbol{X}^{k+1} - \boldsymbol{X}\right)_{\mathcal{T}^{k+1}} \|_{\mathrm{F}}^2 + \| \left(\boldsymbol{X}^{k+1} - \boldsymbol{X}\right)_{\mathcal{T}\setminus\mathcal{T}^{k+1}} \|_{\mathrm{F}}^2 \\
&= \| \left(\boldsymbol{X}^k + \boldsymbol{H}^\top \left(\boldsymbol{Y} - \boldsymbol{H}\boldsymbol{X}^k\right) - \boldsymbol{X}\right)_{\mathcal{T}^{k+1}} \|_{\mathrm{F}}^2 + \| \left(\boldsymbol{X}^{k+1} - \boldsymbol{X}\right)_{\mathcal{T}\setminus\mathcal{T}^{k+1}} \|_{\mathrm{F}}^2 \\
&\leq \| \left(\boldsymbol{X}^k + \boldsymbol{H}^\top \left(\boldsymbol{Y} - \boldsymbol{H}\boldsymbol{X}^k\right) - \boldsymbol{X}\right)_{\mathcal{T}^{k+1}} \|_{\mathrm{F}}^2 \\
&\qquad + 2 \| \left(\boldsymbol{X}^k - \boldsymbol{X} + \boldsymbol{H}^\top \left(\boldsymbol{Y} - \boldsymbol{H}\boldsymbol{X}^k\right)\right)_{\mathcal{T}\Delta\mathcal{T}^{k+1}} \|_{\mathrm{F}}^2 \\
&\leq 3 \| \left(\boldsymbol{X}^k - \boldsymbol{X} + \boldsymbol{H}^\top \left(\boldsymbol{Y} - \boldsymbol{H}\boldsymbol{X}^k\right)\right)_{\mathcal{T}\cup\mathcal{T}^{k+1}} \|_{\mathrm{F}}^2.
\end{aligned}$$

Considering $\boldsymbol{Y} = \boldsymbol{H}\boldsymbol{X} + \boldsymbol{N}$, we then have

$$\begin{aligned}
\|\boldsymbol{X}^{k+1} - \boldsymbol{X}\|_{\mathrm{F}} &\leq \sqrt{3} \| \left(\boldsymbol{X}^k - \boldsymbol{X} + \boldsymbol{H}^\top \left(\boldsymbol{Y} - \boldsymbol{H}\boldsymbol{X}^k\right)\right)_{\mathcal{T}\cup\mathcal{T}^{k+1}} \|_{\mathrm{F}} \\
&= \sqrt{3} \| \left(\left(\boldsymbol{I} - \boldsymbol{H}^\top\boldsymbol{H}\right)\left(\boldsymbol{X}^k - \boldsymbol{X}\right) + \boldsymbol{H}^\top\boldsymbol{N}\right)_{\mathcal{T}\cup\mathcal{T}^{k+1}} \|_{\mathrm{F}} \\
&\leq \sqrt{3} \| \left(\left(\boldsymbol{I} - \boldsymbol{H}^\top\boldsymbol{H}\right)\left(\boldsymbol{X}^k - \boldsymbol{X}\right)\right)_{\mathcal{T}\cup\mathcal{T}^{k+1}} \|_{\mathrm{F}} + \sqrt{3} \| \left(\boldsymbol{H}^\top\boldsymbol{N}\right)_{\mathcal{T}\cup\mathcal{T}^{k+1}} \|_{\mathrm{F}} \\
&\leq \sqrt{3}\delta_{3s} \|\boldsymbol{X}^k - \boldsymbol{X}\|_{\mathrm{F}} + \sqrt{3(1+\delta_{2s})} \|\boldsymbol{N}\|_{\mathrm{F}},
\end{aligned}$$

where the last step is the direct consequence of Lemma 3 and Lemma 4. To see this, we note

$$\begin{aligned}
\| \left(\left(\boldsymbol{I} - \boldsymbol{H}^\top\boldsymbol{H}\right)\left(\boldsymbol{X}^k - \boldsymbol{X}\right)\right)_{\mathcal{T}\cup\mathcal{T}^{k+1}} \|_{\mathrm{F}}^2 &= \sum_n \| \left(\left(\boldsymbol{I} - \boldsymbol{H}^\top\boldsymbol{H}\right)[\boldsymbol{X}^k - \boldsymbol{X}]_n\right)_{\mathcal{T}\cup\mathcal{T}^{k+1}} \|_2^2 \\
&\leq \delta_{3s}^2 \sum_n \|[\boldsymbol{X}^k - \boldsymbol{X}]_n\|_2^2 = \delta_{3s}^2 \|\boldsymbol{X}^k - \boldsymbol{X}\|_{\mathrm{F}}^2,
\end{aligned}$$

where $[\boldsymbol{X}^k - \boldsymbol{X}]_n$ is the nth column of matrix $\boldsymbol{X}^k - \boldsymbol{X}$. We can derive similar argument for $\sqrt{1+\delta_{2s}}\|\boldsymbol{N}\|_{\mathrm{F}}$. Conclusion for HTP has been given in Blanchard et al. (2014, Theorem 3). This concludes the proof.

□

Lemma 6. *For the sparse recovery problem in the stage of unfolding jth ($j \leq I-1$) mode of tensor*

$$\mathbf{T} = \mathbf{X} \times_1 \boldsymbol{H}_1 \times_2 \boldsymbol{H}_2 \cdots \times_j \boldsymbol{H}_j \times_{j+1} \boldsymbol{I}_{N_{j+1}} \cdots \times_I \boldsymbol{I}_{N_I} + \mathbf{N},$$

where the sparse tensor $\mathbf{X}$ corresponds to s standard sparse $\boldsymbol{x}$ or s hierarchically sparse $\boldsymbol{x}$. Its jth mode unfolding leads to

$$\boldsymbol{T}_{(j)} = \boldsymbol{H}_j\boldsymbol{U}_j + \boldsymbol{N}_{(j)} = \boldsymbol{H}_j\boldsymbol{X}_{(j)} \left(\boldsymbol{I}_{\prod_{i=I}^{j+1} N_i} \otimes \left(\otimes_{i=j-1}^{1} \boldsymbol{H}_i\right)\right)^\top + \boldsymbol{N}_{(j)}. \tag{6}$$

Then the estimate of $\boldsymbol{U}_j$, denoted as $\tilde{\boldsymbol{U}}_j$ and obtained through IHT or HTP, satisfies

$$\|[\tilde{\boldsymbol{U}}_j]_{\mathrm{n_{j+1}}} - [\boldsymbol{U}_j]_{\mathrm{n_{j+1}}}\|_{\mathrm{F}} \leq \alpha_j^k \|[\boldsymbol{U}_j]_{\mathrm{n_{j+1}}}\|_{\mathrm{F}} + \tau_j \|[\tilde{\boldsymbol{U}}_{j+1} - \boldsymbol{U}_{j+1}]_{\mathrm{n_{j+2}}}\|_{\mathrm{F}}, \tag{7}$$

where $[\tilde{\boldsymbol{U}}_j]_{\mathrm{n_{j+1}}}$ *and* $[\boldsymbol{U}_j]_{\mathrm{n_{j+1}}} := [\boldsymbol{X}_{(j)}]_{\mathrm{n_{j+1}}} \left(\otimes_{i=j-1}^{1} \boldsymbol{H}_i\right)^\top$ *denote the* $\mathrm{n_{j+1}}$*th column block of* $\tilde{\boldsymbol{U}}_j$ *and* $\boldsymbol{U}_j$*, respectively. Here, encapsulation* $\mathrm{n_{j+1}} := (n_{j+1}, \cdots, n_{I-1}, n_I)$ *is the index for the column block. The indices* $\{n_i\}_{i=j+2}^{I}$ *in encapsulation* $\mathrm{n_{j+2}} := (n_{j+2}, \cdots, n_{I-1}, n_I)$ *have the same value as the indices* $\{n_i\}_{i=j+2}^{I}$ *in encapsulation* $\mathrm{n_{j+1}}$*, i.e., the block indexed by* $\mathrm{n_{j+2}}$ *should be a parent block of the block indexed by* $\mathrm{n_{j+1}}$*. Constants* μ_j *and* τ_j *depend on the iteration number* k *and matrix* $\boldsymbol{H}_j$*.*

Proof. According to Lemma 1, we solve Equation 6 by separating it into $\prod_{i=I}^{j+1} N_i$ MMV problem, where each MMV problem is indexed by an encapsulation $\mathrm{n_{j+1}}$. Suppose we consider a fixed encapsulation $\mathrm{n}^*_{\mathrm{j+1}} = (n^*_{j+1}, \cdots, n^*_I)$, and consider the MMV problem indexed by $\mathrm{n}^*_{\mathrm{j+1}}$ as

$$[\boldsymbol{T}_{(j)}]_{\mathrm{n}^*_{\mathrm{j+1}}} = \boldsymbol{H}_j [\boldsymbol{U}_j]_{\mathrm{n}^*_{\mathrm{j+1}}} + [\boldsymbol{N}_{(j)}]_{\mathrm{n}^*_{\mathrm{j+1}}} = \boldsymbol{H}_j [\boldsymbol{X}_{(j)}]_{\mathrm{n}^*_{\mathrm{j+1}}} \left(\otimes_{i=j-1}^{1} \boldsymbol{H}_i\right)^\top + [\boldsymbol{N}_{(j)}]_{\mathrm{n}^*_{\mathrm{j+1}}}.$$

According to Lemma 5 and denoting the solution as $[\tilde{\boldsymbol{U}}_j]_{\mathrm{n}^*_{\mathrm{j+1}}}$ with k IHT or HTP iterations, we have

$$\|[\tilde{\boldsymbol{U}}_j]_{\mathrm{n}^*_{\mathrm{j+1}}} - [\boldsymbol{U}_j]_{\mathrm{n}^*_{\mathrm{j+1}}}\|_{\mathrm{F}} \leq \alpha_j^k \|[\boldsymbol{U}_j]_{\mathrm{n}^*_{\mathrm{j+1}}}\|_{\mathrm{F}} + \tau_j \|[\boldsymbol{N}_{(j)}]_{\mathrm{n}^*_{\mathrm{j+1}}}\|_{\mathrm{F}},$$

where μ_j and τ_j relate to the RICs of matrix $\boldsymbol{H}_j$. The only step left is to bound $\|[\boldsymbol{N}_{(j)}]_{\mathrm{n}^*_{\mathrm{j+1}}}\|_{\mathrm{F}}$ using $[\boldsymbol{E}_{j+1}]_{\mathrm{n}^*_{\mathrm{j+2}}}$, where $E_{j+1} = \tilde{\boldsymbol{U}}_{j+1} - \boldsymbol{U}_{j+1}$.

We recall that Equation 6 is obtained by unfolding the measurement tensor formed from the matrix $\tilde{\boldsymbol{U}}_{j+1} = \boldsymbol{U}_{j+1} + \boldsymbol{E}_{j+1}$ along its jth mode. Hence, $\boldsymbol{N}_{(j)}$ is simply reordered version of $\boldsymbol{E}_{j+1}$. Consequently, the entries of the matrix $[\boldsymbol{N}_{(j)}]_{\mathrm{n}^*_{\mathrm{j+1}}}$ are essentially entries of the n^*_{j+1}th row of $[\boldsymbol{E}_{j+1}]_{\mathrm{n}^*_{\mathrm{j+2}}}$, leading to

$$\|[\boldsymbol{N}_{(j)}]_{\mathrm{n}^*_{\mathrm{j+1}}}\|_{\mathrm{F}} \leq \|[\boldsymbol{E}_{j+1}]_{\mathrm{n}^*_{\mathrm{j+2}}}\|_{\mathrm{F}},$$

and we arrive at the desired result.

To elaborate, we first investigate the indices of the entries of $[\boldsymbol{N}_{(j)}]_{\mathrm{n}^*_{\mathrm{j+1}}}$. The entries of the n^*_jth row of matrix $[\boldsymbol{N}_{(j)}]_{\mathrm{n}^*_{\mathrm{j+1}}}$ are obtained by i) fixing $n_j = n^*_j$ (row index) and $n_{j+1} = n^*_{j+1}, \cdots, n_I = n^*_I$ (encapsulation), and ii) running $n_1, \cdots, n_{j-1}$ from one till $N_1, \cdots, N_{j-1}$, respectively. Thus, the entries of matrix $[\boldsymbol{N}_{(j)}]_{\mathrm{n}^*_{\mathrm{j+1}}}$ can be obtained by i) fixing $n_{j+1} = n^*_{j+1}, \cdots, n_I = n^*_I$, ii) running $n_1, \cdots, n_{j-1}$ from one till $N_1, \cdots, N_{j-1}$, respectively, and iii) running $n_j = 1, \cdots, N_j$ (going over all rows). Given such knowledge, we start investigating the n^*_{j+1}th row of matrix $[\boldsymbol{E}_{j+1}]_{\mathrm{n}^*_{\mathrm{j+2}}}$. The entries of this row are obtained by i) fixing $n_{j+1} = n^*_{j+1}$ (row index), ii) fixing $n_{j+2} = n^*_{j+2}, \cdots, n_I = n^*_I$ (fixed encapsulation), and iii) running $n_1, \cdots, n_j$ from one till $N_1, \cdots, N_j$, respectively. By comparing how indices are arranged, we can see that the entries of the matrix $[\boldsymbol{N}_{(j)}]_{\mathrm{n}^*_{\mathrm{j+1}}}$ are essentially entries of the n^*_{j+1}th row of $[\boldsymbol{E}_{j+1}]_{\mathrm{n}^*_{\mathrm{j+2}}}$, inferring $\|[\boldsymbol{N}_{(j)}]_{\mathrm{n}^*_{\mathrm{j+1}}}\|_{\mathrm{F}} \leq \|[\boldsymbol{N}_{j+1}]_{\mathrm{n}^*_{\mathrm{j+2}}}\|_{\mathrm{F}}$. □

As we have described before, Equation 6 is solved through multiple independent MMV problems. Thus, the error bound is also given regarding each individual MMV problem. Further, not only the jth step, but also the $j+1$th step is solved through multiple independent MMV problems. Thus, we do not have the upper bound for $\boldsymbol{E}_{j+1}$ in Equation 4 as a whole but only the upper bound for each column block $[\boldsymbol{E}_{j+1}]_{\mathrm{n_{j+2}}}$. Fortunately, since all the noise entries in the jth step are contained as one single row of the noise block in the previous step, having the upper bound for each column block $[\boldsymbol{E}_{j+1}]_{\mathrm{n_{j+2}}}$ is sufficient to derive the noise bound for the jth step, which is shown in Lemma 6 and Equation 7.

Now, we proceed to the proof of Theorem 2. Generally speaking, Theorem 2 is obtained by recursively applying Lemma 6. Particularly, focusing on the $\boldsymbol{s}$ hierarchical sparse vectors, for the last step, i.e., *the first mode unfolding*, we solve

$$\boldsymbol{T}_{(1)} = \boldsymbol{H}_1 \boldsymbol{X}_{(1)} + \boldsymbol{N}_{(1)},$$

leading to $\prod_{j=2}^{I} N_j$ SMV problems. They are SMV because there is only one column in each column block, and hence the MMV problem reduces to the SMV problem. Lemma 6 indicates that

$$\begin{aligned}\|\tilde{\boldsymbol{U}}_1 - \boldsymbol{U}_1\|_{\mathrm{F}} &\leq \sum_{n_2,\cdots,n_I} \|[\tilde{\boldsymbol{U}}_1]_{\mathrm{n}_2} - [\boldsymbol{U}_1]_{\mathrm{n}_2}\|_{\mathrm{F}} \leq \sum_{n_2,\cdots,n_I} \alpha_1^k \|[\boldsymbol{U}_1]_{\mathrm{n}_2}\|_{\mathrm{F}} + \tau_1 \|[\boldsymbol{E}_2]_{\mathrm{n}_3}\|_{\mathrm{F}} \\ &\leq \sum_{n_2,\cdots,n_I} \alpha_1^k \|[\boldsymbol{U}_1]_{\mathrm{n}_2}\|_{\mathrm{F}} + \tau_1 \left(\alpha_2^k \|[\boldsymbol{U}_2]_{\mathrm{n}_3}\|_{\mathrm{F}} + \tau_2 \|[\boldsymbol{E}_3]_{\mathrm{n}_4}\|_{\mathrm{F}}\right) \\ &\leq \sum_{n_2,\cdots,n_I} \left(\sum_{i=1}^{I} \prod_{j=1}^{i-1} \tau_j \alpha_i^k \left\|[\boldsymbol{U}_i]_{\mathrm{n}_{i+1}}\right\|_{\mathrm{F}} + \prod_{i=1}^{I} \tau_i \|[\boldsymbol{E}_I]_{\mathrm{n}_{I+1}}\|_{\mathrm{F}} \right).\end{aligned}$$

We note that $I+1$th level contains only one block, leading to $[\boldsymbol{E}_I]_{\mathrm{n}_{I+1}} = \boldsymbol{E}_I$. Using the relation $\tilde{\boldsymbol{U}}_I = \boldsymbol{U}_I + \boldsymbol{E}_I$ and Lemma 5 leads to $\|\boldsymbol{E}_I\|_{\mathrm{F}} \leq \alpha_I^k \|\boldsymbol{U}_I\|_{\mathrm{F}} + \tau_I \|\boldsymbol{N}_{(1)}\|_{\mathrm{F}}$. This concludes the proof for $\boldsymbol{s}$ hierarchical sparsity. For s standard sparsity, the upper bound for all s standard sparse vectors is the worst upper bound among all possible $\boldsymbol{s}$ corresponding to the sparsity level s. Therefore, taking the maximum over $\forall \boldsymbol{s} \in f_{\mathrm{N}}(s)$ concludes the proof.

For $\boldsymbol{s}$ Kronecker-supported sparsity, since the support is shared among different blocks in the same level, it is unnecessary to introduce multiple MMV problems, but to solve only one MMV problem. Thus, recursively applying Lemma 5 leads to the final result. For the last step, we solve

$$\boldsymbol{T}_{(1)} = \boldsymbol{H}_1 \boldsymbol{X}_{(1)} + \boldsymbol{N}_{(1)},$$

which leads to the following relations,

$$\begin{aligned}\|\tilde{\boldsymbol{U}}_1 - \boldsymbol{U}_1\|_{\mathrm{F}} &\leq \alpha_1^k \|\boldsymbol{U}_1\|_{\mathrm{F}} + \tau_1 \|\boldsymbol{N}_{(1)}\|_{\mathrm{F}} \\ &\leq \alpha_1^k \|\boldsymbol{X}_{(1)}\|_{\mathrm{F}} + \tau_1 \left(\alpha_2^k \|\boldsymbol{U}_2\|_{\mathrm{F}} + \tau_2 \|\boldsymbol{N}_{(2)}\|_{\mathrm{F}}\right) \\ &\leq \sum_{i=1}^{I} \prod_{j=1}^{i-1} \alpha_i^k \tau_j \|\boldsymbol{U}_i\|_{\mathrm{F}} + \prod_{i=1}^{I} \tau_i \|\boldsymbol{\mathsf{N}}\|_{\mathrm{F}}.\end{aligned}$$

Thus, the proof is complete.

G Additional Numerical Evaluations

This section presents a more comprehensive evaluation of our MSR framework, consisting of complete results of Section 5 and a new set of results where we vary the number of measurements with a fixed SNR. We also include a new metric named support recovery rate (SRR) defined as

$$\mathrm{SRR} = \frac{|\operatorname{supp}(\hat{\boldsymbol{x}}) \cap \operatorname{supp}(\boldsymbol{x})|}{|\operatorname{supp}(\hat{\boldsymbol{x}}) \cup \operatorname{supp}(\boldsymbol{x})|},$$

where $\operatorname{supp}(\cdot)$ returns the set of positions of the nonzero entries of the argument vector, $|\cdot|$ returns the cardinality of the argument set, $\hat{\boldsymbol{x}}$ is the estimated sparse vector, and $\boldsymbol{x}$ is the groundtruth.

We show a complete version of Figure 2 in Figure 5. We use Tensorlab (Vervliet et al., 2016) for tensor operation and `Seq` and `Pl` to represent the *sequential* and *parallel* (`parfor` function in Matlab (Inc., 2024)) implementation of Equation 5; they have the same recovery performance but different run times. In the recovery of s standard sparse vectors, compared to Figure 2a, Figure 5a includes both the sequential and parallel implementation of our MSSBL. Regardless of different run times as in Table 3, sequential and parallel implementations provide identical NSE and SRR results. Regarding run time, only in low SNR cases, MSSBL-`Pl` is faster than MSSBL-`Seq`. This is because in high SNR cases, the parallel overhead dominates, including data transfer and communication cost. As we see in Figure 3, when the computation cost dominates, there is a significant gain in computation time, as a trade-off for memory usage. In the recovery of $\boldsymbol{s}$ hierarchical sparse vectors, compared to Figure 2b, Figure 5b includes the performance of MSSBL. MSSBL exhibits a worse performance in low SNR scenario because it does not require the true sparsity level $\boldsymbol{s}$ as an input, while for IHT/HTP-based algorithms, this prior knowledge is necessary. However, MSSBL is still able to offer a comparable performance in high SNR scenarios, making it a powerful candidate

Table 3: Averaged run time. A complete version of Table 1. **Bold**: the best result.

SNR	3 dB	7 dB	11 dB	15 dB	19 dB	23 dB
Recovery of s sparse vectors						
MSOMP-Seq	**0.4256**	**0.4119**	0.3827	0.3329	0.2204	**0.0568**
KroOMP	130.5405	108.0526	76.6942	39.9844	11.5774	0.7525
MSSBL-Seq	1.8191	1.1016	0.5758	**0.2218**	**0.1417**	0.1141
MSSBL-Pl	0.4517	4.9263	**0.2658**	1.8292	0.1531	0.1281
Recovery of $\boldsymbol{s}$ hierarchically sparse vectors						
MSSBL-Seq	2.4930	2.0134	1.2501	0.6102	0.1965	0.1112
MSSBL-Pl	0.4962	0.4607	1.3664	0.2513	0.1447	0.1081
MSHTP-Seq	**0.0379**	**0.0305**	**0.0297**	**0.0247**	**0.0186**	**0.0168**
HiHTP	0.6512	0.5493	0.5204	0.5444	0.4398	0.4574
HTP	2.2436	1.7170	1.3256	0.8450	0.8264	0.5311
MSIHT-Seq	0.0500	0.0510	0.0532	0.0509	0.0450	0.0434
IHT	8.2437	8.2412	8.2554	8.2917	8.2889	8.2789
Recovery of $\boldsymbol{s}$ Kronecker-supported sparse vectors						
MSOMP	0.0042	0.0041	0.0040	0.0038	0.0026	0.0015
MSHTP	0.0011	0.0010	0.0011	0.0010	0.0010	0.0010
MSSBL	0.0728	0.0587	0.0447	0.0279	0.0119	0.0051
SVD-KroSBL	37.1233	26.9816	14.2405	8.6036	5.4067	4.0681
AM-KroSBL	55.9532	63.4676	75.9727	74.5840	51.7089	34.1331
HTP	0.9772	0.8347	0.4709	0.3465	0.2339	0.2323
MSIHT	**0.0008**	**0.0007**	**0.0007**	**0.0007**	**0.0007**	**0.0007**
IHT	6.0771	6.0760	6.0763	6.0690	6.0677	6.0535
KSHTP	0.1018	0.0730	0.0665	0.0811	0.0865	0.0881

when the prior knowledge $\boldsymbol{s}$ is absent. In the recovery of $\boldsymbol{s}$ Kronecker-supported sparse vectors, compared to Figure 2c, we include IHT/HTP-based algorithms in Figure 5c. KSHTP is the algorithm we explained in Equation HTP. Although the thresholding operator for Kronecker support is not optimal, KSHTP still offers the best SRR performance, followed by MSHTP. MSIHT has the least run time, which is four orders less than its classic counterpart IHT. Overall, Figure 5 and Table 3 demonstrate that our MSR framework can offer comparable or better performance with significantly reduced run time.

We next evaluate the performance of different algorithms by fixing the SNR and varying the number of measurements. The setting is as follows. For the s standard sparsity, we opt for $\boldsymbol{H} = \otimes_{i=I}^{1} \boldsymbol{H}_i$ with $I = 2$, and set $M = \{48, 52, 56, \cdots, 72\}$ and $N = 80$. The entries of $\boldsymbol{H}_i$ and nonzero entries of $\boldsymbol{x}$ are drawn independently from the standard normal distribution. We set $s = 15$, and the support is randomly drawn from a uniform distribution. For $\boldsymbol{s}$ hierarchically sparse vectors, we also opt for $I = 2$, and set $M = \{48, 52, 56, \cdots, 72\}$, $N = 80$, and $s = 15$. In the Kronecker-supported sparsity model, we opt for $I = 3$, and set $M = \{12, 13, \cdots, 16\}$, $N = 18$, and $s = 4$. We adopt the additive white Gaussian noise with zero mean with SNR (dB) $= 20$. Ratio is defined as $\bar{M}/\bar{N} = \prod_{i=1}^{I} M_i/N_i = (M/N)^I$. We consider NSE, SRR, and run time for performance evaluation. We follow the same way to cap the number of iterations. Results in Figure 6 and Table 4 are obtained through two hundred independent trials. Overall, we observe similar trends as in Figure 5 and Table 3. Our MSR is able to provide comparable or better performance with reduced run time, demonstrating the efficacy of exploiting the Kronecker product structure in the recovery process.

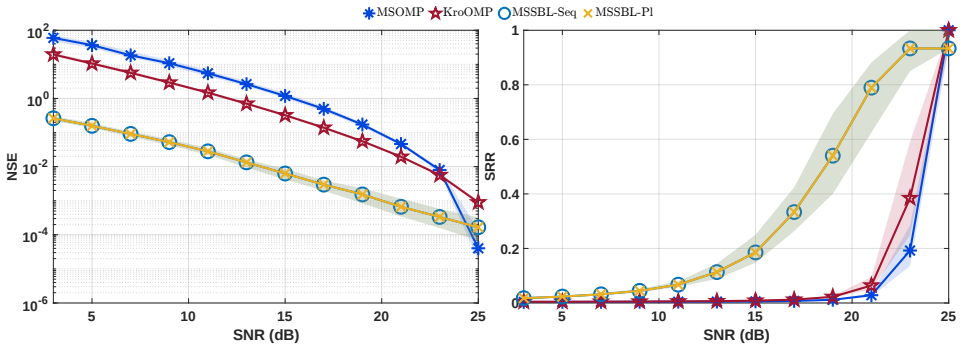

(a) s standard sparsity.

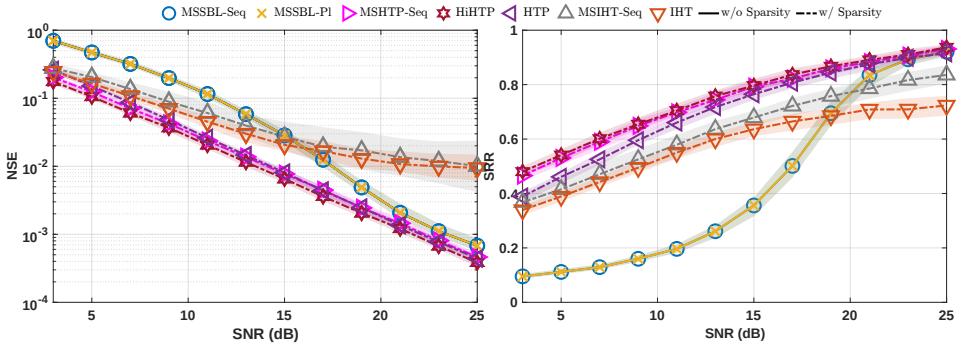

(b) $\boldsymbol{s}$ hierarchically sparsity.

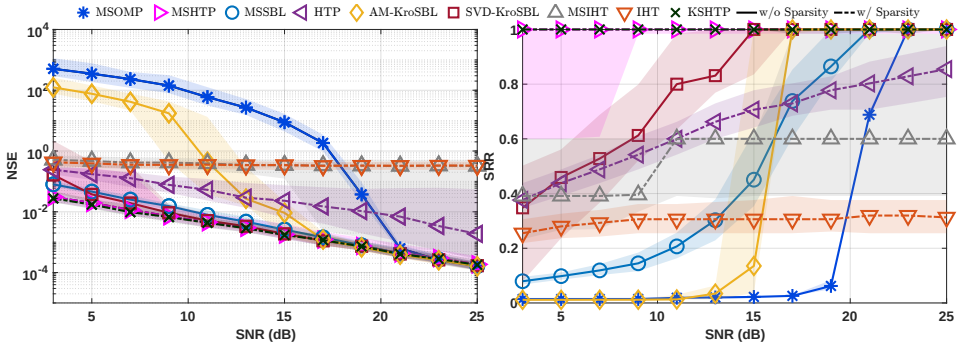

(c) $\boldsymbol{s}$ Kronecker-supported sparsity.

Figure 5: NSE and SRR as functions of SNR.

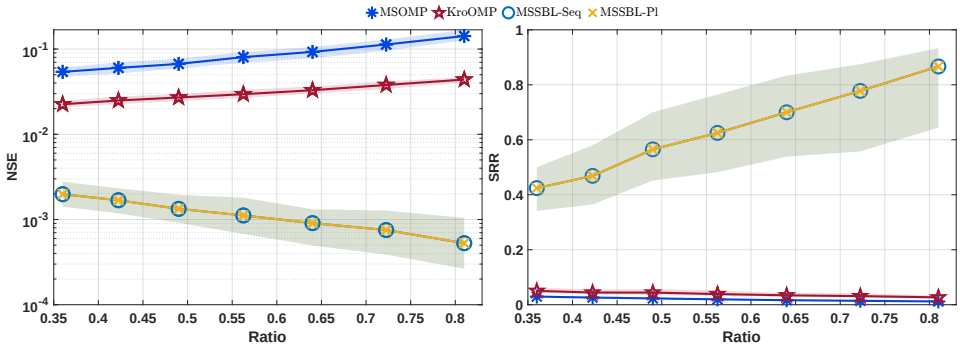

(a) s standard sparsity.

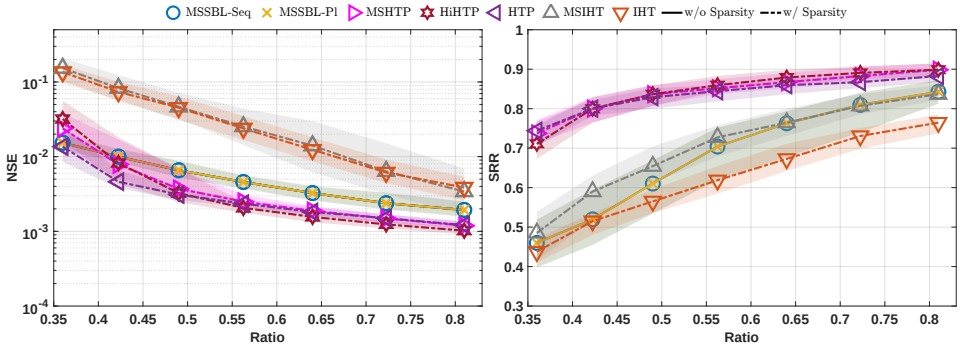

(b) $\boldsymbol{s}$ hierarchically sparsity.

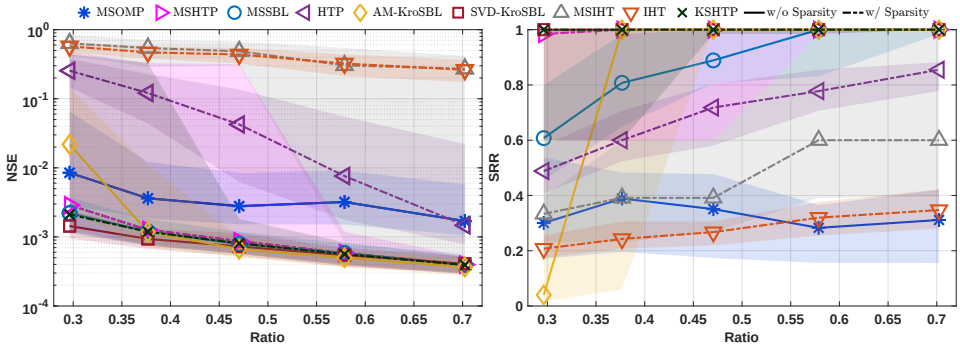

(c) $\boldsymbol{s}$ Kronecker-supported sparsity.

Figure 6: NSE and SRR as functions of the number of measurements.

Table 4: Averaged runtime in seconds. **Bold**: the best result.

Recovery of s sparse vectors							
M	48	52	56	60	64	68	72
MSOMP-Seq	**0.0735**	**0.0951**	**0.1265**	0.1574	0.1937	0.2312	0.2918
KroOMP	0.7139	1.1941	2.1137	3.7952	7.4092	12.5439	22.4149
MSSBL-Seq	0.1726	0.1743	0.1439	**0.1364**	**0.1332**	**0.1368**	**0.1321**
MSSBL-Pl	0.1412	0.1464	0.1508	0.1517	0.1498	0.1527	0.3298

Recovery of $\boldsymbol{s}$ hierarchically sparse vectors							
M	48	52	56	60	64	68	72
MSSBL-Seq	0.2978	0.2594	0.2031	0.1692	0.1552	0.1407	0.1274
MSSBL-Pl	0.1734	0.1614	0.1467	0.1363	0.1299	0.1248	0.1197
MSHTP-Seq	**0.0204**	**0.0198**	**0.0190**	**0.0191**	**0.0178**	**0.0170**	**0.0168**
HiHTP	0.3661	0.3622	0.3691	0.4189	0.4181	0.4599	0.5127
HTP	0.3071	0.3641	0.4753	0.4980	0.6407	0.6867	0.4566
MSIHT-Seq	0.0527	0.0502	0.0479	0.0457	0.0449	0.0421	0.0416
IHT	4.7097	5.4549	6.2188	7.1292	8.3298	9.1231	10.1874

Recovery of $\boldsymbol{s}$ Kronecker-supported sparse vectors					
M	12	13	14	15	16
MSOMP	0.0017	0.0017	0.0019	0.0020	0.0023
MSHTP	0.0010	0.0010	0.0011	0.0011	0.0013
MSSBL	0.0187	0.0141	0.0118	0.0092	0.0083
SVD-KroSBL	5.3134	4.8928	4.7247	5.0780	5.3094
AM-KroSBL	52.0891	52.4779	49.6836	47.0243	42.6749
HTP	0.0715	0.1113	0.1658	0.2508	0.2745
MSIHT	**0.0009**	**0.0008**	**0.0009**	**0.0007**	**0.0007**
IHT	3.4581	4.0502	4.9489	6.0187	7.2859
KSHTP	0.1184	0.0908	0.1048	0.0885	0.0829